NKS-505
ISBN 978-87-7893-603-5

Symmetrical Array Methodology for Gamma Source Localization: Technology Transfer Workshop and Field Event (SAMLOC)

Harri Toivonen[1] Mark Dowdall[2] Sakari Ihantola[3] Gísli Jónsson[4], Pernille Ahlmann Jensen[4] Jussi Huikari[5], Kari Peräjärvi[5], Philip Holm[5] Aliaksandr Dvornik[6], Maria Karampiperi[6], Christopher Rääf[6], Viktor Lehmann[6], Robert Finck[6], Christian Bernhardsson[6]

[1]HT Nuclear Oy, 05880 Hyvinkää, Finland,
[2]Norwegian Radiation and Nuclear Safety Authority, 1361, Østerås, Norway,
[3]Radis Technologies Oy, Finland,
[4]Icelandic Radiation safety Authority, 105 Reykjavík, Iceland,
[5]Radiation and Nuclear Safety Authority, 01370 Vantaa, Finland,
[6]Lund University, Malmö, Sweden

October 2025

Abstract

Effective response to incidents involving searches for nuclear or other radioactive materials out of regulatory control (MORC) is dependent on rapid localization of the source, which is often hindered due to a general lack of available, efficient, robust directionally sensitive detector systems designed for field and security applications. The SAMLOC project assembled Nordic expertise in this area to test new developments, exchange technologies and experience and enhance Nordic capacities in this field. The primary objective of SAMLOC was is to investigate the application of the symmetrical array method to detector types employed in the Nordic region and to test this and conventional methods in tests of directional estimation. The project demonstrated that simple models, developed for rectangular and cylindrical detector geometries, explain well the directional data acquired with 2x1 arrays of detectors. The models function well for large detectors which provide inherent attenuation of photons in the front detector, preventing them reaching the back detector. A shield of 4 cm Pb between detectors was sufficient for a good directional response. Comparison measurements were performed between 2x1 and 2x2 arrays. The latter was technically superior having 360 degrees field of view, and there was no need to perform any modelling of the array. However, a 2x1 array is technically much simpler and cheaper, albeit with lower directional accuracy. The array is well suited for static surveillance of an area of interest and is of relevance in nuclear security applications.

Key words

Gamma spectrometry, detector arrays, source locations, directionality

NKS-505
ISBN 978-87-7893-603-5
Electronic report, October 2025
NKS Secretariat
P.O. Box 49
DK - 4000 Roskilde, Denmark
Phone +45 4677 4041
www.nks.org
e-mail nks@nks.org

Symmetrical Array Methodology for Gamma Source Localization: Technology Transfer Workshop and Field Event (SAMLOC)

Final Report from the NKS-B SAMLOC activity (Contract: AFT/B(24)4)

Harri Toivonen[1]
Mark Dowdall[2]
Sakari Ihantola[3]
Gísli Jónsson[4], Pernille Ahlmann Jensen[4]
Jussi Huikari[5], Kari Peräjärvi[5], Philip Holm[5]
Aliaksandr Dvornik[6], Maria Karampiperi[6], Christopher Rääf[6], Viktor Lehmann[6], Robert Finck[6] , Christian Bernhardsson[6]

[1] HT Nuclear Oy, 05880 Hyvinkää, Finland
[2] Norwegian Radiation and Nuclear Safety Authority, 1361, Østerås, Norway
[3] Radis Technologies Oy, Finland
[4] Icelandic Radiation safety Authority, 105 Reykjavík, Iceland
[5] Radiation and Nuclear Safety Authority, 01370 Vantaa, Finland
[6] Lund University, Department of Translational Medicine (ITM), Malmö, Sweden

Table of contents

1. Introduction

Incidents involving searches for nuclear or other radioactive materials out of regulatory control (MORC) are common and contextually varied ranging from lost industrial, medical or other sources to the response to, or prevention of, illicit trafficking or malicious use of radioactive materials. A commonality is that search operations for MORC require the utilization of significant resources in the form of ground-based systems (car or person borne detection, static scanning etc.) or aerial systems (helicopter, fixed wing or drone mounted) over wide areas and often for extended periods of time. Estimation of the direction to a source and its subsequent localization is crucial for operations to return the source to regulatory control. Conventionally, estimates of the direction to a source are provided with detection instruments delivering real-time readings of the strength of the prevailing radiation field. Such instruments may be dose rate meters, plastic counters or spectrometers operating typically on the principle that the higher the reading, the shorter the distance to the source. This approach is tedious, error prone and often involves serious safety and security issues. More capable instruments are required for more efficient, safe and reliable information provision with respect to the direction to a source and the vast majority of available instruments fall within or rely upon the following general categories: collimators and imagers (Toivonen et al., 2023). Consideration of detection systems providing estimates of directionality indicates that the vast majority of systems are subject to weaknesses in two specific aspects with respect to suitability for field operations. The first of these is that the detection instruments employed are often of low intrinsic efficiency, are of small size and may not be “off the shelf” components. The second is in relation to their implementation. Detection systems where additional mechanical systems are employed – for rotation of detectors or collimators – or where detector elements are mounted on adjustable jigs or other constructions to maintain specific orientations are not ideal for field operations. Similarly, complex interactive analysis routines applied to the data either in real time or for the purposes of post-processing later, do not lend themselves to field operations where rapid response is of importance.

A system that eliminates all of the problems associated with previous attempts to provide directionality capabilities to field instrument has recently been developed (Toivonen et al., 2024). In essence, the system relies upon using the geometrical centres of individual detector elements of a symmetrical detector array as surrogates for the interaction locations of photons with the elements. The system is scalable in terms of array element size and materials, applicable to standard detector types and capable of providing direction estimates to within a few degrees using either the primary photopeak or scattered photons from partially shielded sources. The method has been extensively assessed using simulation methods and a prototype has been built (Sakari Ihantola, Finland) and tested at STUK.

The new source localization system is such that it is possible to apply standard detectors, i.e., a functional system can be assembled from existing detectors without permanent changes to hardware. The primary objective of the SAMLOC proposal is to investigate the application of the symmetrical array method to detector types employed in the Nordic region, in configurations amenable to most organisations and to test this and conventional methods in laboratory tests of directional estimation. Secondary objectives include an opportunity for technology transfer between Nordic experts on the matter of directionally sensitive gamma detectors and the establishment of a common, easily implemented, non-commercial methodology and platform to improve search and response capacities in incidents involving searches for MORC in the Nordic area.

2. Directional sensitivity of a 2x1 array: Technical foundation

In an array of detectors any individual detector element functions as a radiation shield for other elements in the array. This phenomenon can be used to design a directionally sensitive array (DSA), and indeed such work has been carried out successfully, in particular for 2x2 arrays (Toivonen et al 2024). The self-occlusion principle should potentially work also for the smallest array comprised of only two adjacent detector elements. Shirakawa et al. (2009) described a tandem detector (phoswich) by combining NaI and BGO scintillators, demonstrating that the pulse rates recorded by the anterior and posterior detectors have a directionally sensitive relationship. However, in addition to the angle dependency, the pulse rate ratio has an energy dependency because many of the photons penetrate through the front detector to the back detector, and the magnitude of this penetration depends on the energy of the photons. Therefore, the data analysis of a phoswhich detector is complex. Introducing a shield between the two detectors eliminates most of the photon penetration problem. An ideal 2x1 array would have detectors of large dimension and their housing should be as near as possible to the sensitive element (scintillator). The 2x1 array has a field of view 180 degrees. Therefore, it is best suited for static measurements, such as near a wall facing towards a large area. Figure 2.1 shows the array configuration. The gap between the adjacent detectors creates an insensitive angular interval around the direction perpendicular to the array. A shield between the detectors improves the directional capability in two ways: (1) preventing photons penetrating through the front detector to the back detector and simultaneously (2) the detrimental gap between the surfaces of the detectors is halved, thus reducing the size of the insensitive angular interval. Modern NaI detectors typically have an aluminium housing with a thickness of 1.5 mm and an air gap of 2 mm separating the cover from the scintillator (Scionix). However, there are other designs of NaI detectors where the overall gap around the NaI scintillator exceeds 10 mm. Such a detector housing will cause problems for the directional analysis through the creation of an angle interval where the count ratio of the back and front voxels is constant. In an ideal case, both detectors would be unshielded relative to the source only at the position of symmetry, but because of the gap, there is an insensitive angle interval.

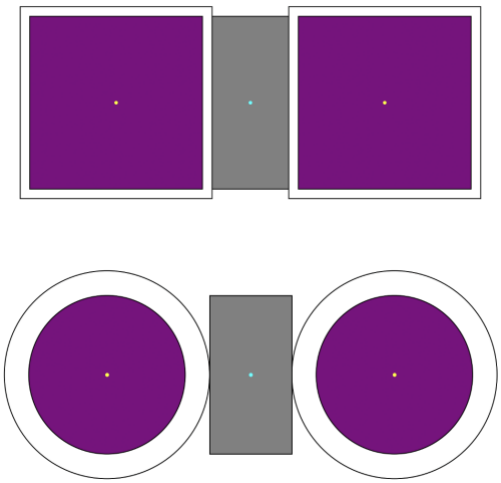

Figure 2.1. Rectangular and cylindrical array having a shield between the detectors. A small gap between the detectors (Al cover and air) is ideal for directional studies.

2.1 Array with a shield between the detectors

Consider two similar detectors of rectangular shape. A radiation shield is placed between the detectors. Figures 2.2 and 2.3 define the measurement system. The ratio of counts in the back (B) and front (F) detectors can be calculated from the geometry of the system. Such an analysis is strictly valid only for low-energy photons (< 60 keV). The geometry of the system is the most dominant variable of the count ratio B/F, and therefore a simple model is warranted to understand the importance of each parameter (dimensions). Monte Carlo calculations can then be performed for the desired photon energy to obtain a more realistic response at larger energies.

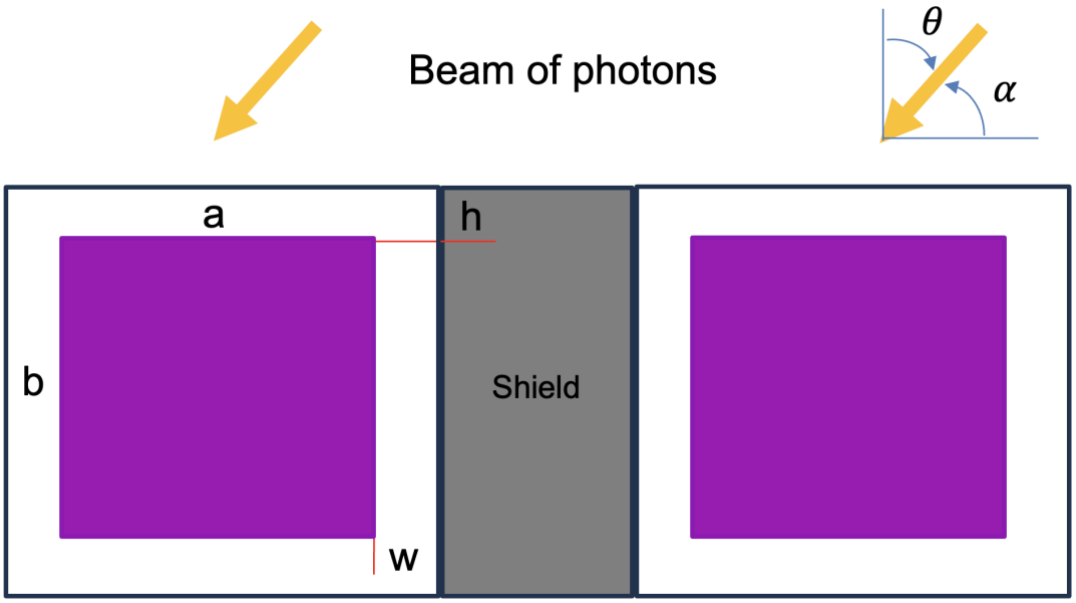

Figure 2.2 Top view of the measurement geometry of a 2x1 rectangular array. A shield (Pb or W) is placed between the detectors which are in separate enclosures. The detectors are identical and have a sensitive cross-sectional area of a x b. There is a gap (w) between the detector sensitive area and the outer surface of the enclosure; the shield may extend beyond the detector surface level creating a small collimator (h) The front detector at the right is always 100 % exposed at positive angles of θ. At negative angles, the front and back detector naming is swapped.

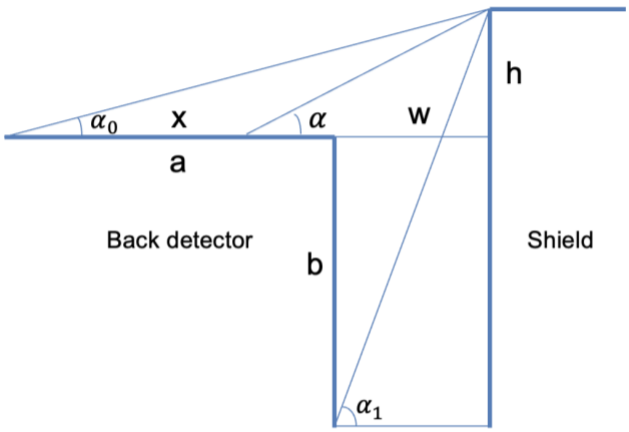

Figure 2.3. Back detector and gap in front of a shield in a 2x1 rectangular array. The back detector is fully shielded when the beam angle is smaller than the angle α_0 and it is fully exposed when the beam angle is larger than α_1.

When the source is far away from the array (> 5 m), it sends a parallel beam of photons towards the array. The ratio of counts in the back and front detectors can be calculated using the geometry shown in Figure 3:

$$R = 0, \quad \alpha < \alpha_0 \qquad [1]$$

$$R = 1, \quad \alpha > \alpha_1 \qquad [2]$$

where:

$$tan\alpha_0 = \frac{h}{a+w} \qquad [3]$$

$$tan\alpha_1 = \frac{b+h}{w} \qquad [4]$$

The count ratio between the angles α_0 and α_1 can be calculated by noting that the front detector exposure is proportional to:

$$I_F = asin\alpha + bcos\alpha \qquad [5]$$

and the back detector exposure is proportional to:

$$I_B = xsin\alpha \qquad [6]$$

where:

$$x = a + w - \frac{h}{tan\alpha} \qquad [7]$$

Therefore, the ratio I_B/I_F is:

$$R = \frac{(a+w)sin\alpha - hcos\alpha}{asin\alpha + bcos\alpha}, \quad \alpha \in [\alpha_0, \alpha_1] \qquad [8]$$

In practise, it is more convenient to define the source direction using the complementary angle $\theta = \frac{\pi}{2} - \alpha$:

$$R = \frac{(a+w)cos\theta - hsin\theta}{acos\theta + bsin\theta} \qquad [9]$$

In an ideal symmetrical case, $a = b$, $h = 0$ and $w = 0$. Then:

$$R = \frac{cos\,(\theta)}{cos(\theta) + sin(\theta)} \qquad [10]$$

Figure 2.4 shows the count ratio R referring to the parameters of a simulated small CZT detector having dimensions of 10 x 10 x 10 mm^3. A shield of tungsten (10 mm) is installed between the detectors. The response is very near the ideal situation when the gap (2 mm) is small between the detector sensitive area and the outer layer of the enclosure. In this case, a directional accuracy of ten degrees can be achieved throughout the direction of 180 degrees. The response is essentially worse when the sensitive area is far away (7.5 mm) from the surface of the detector (Figure 2.5). Extending the tungsten shield to a position above the

surface of the detectors (h = 6 mm) improves the response. However, there is a large insensitive area between the angles of -37 and 37 degrees. For a more precise directional estimate, the measurement should be repeated tilting the array by 45 degrees. Figure 2.6 is a comparison between the geometry model and Geant4 simulations for photon energy of 59 keV.

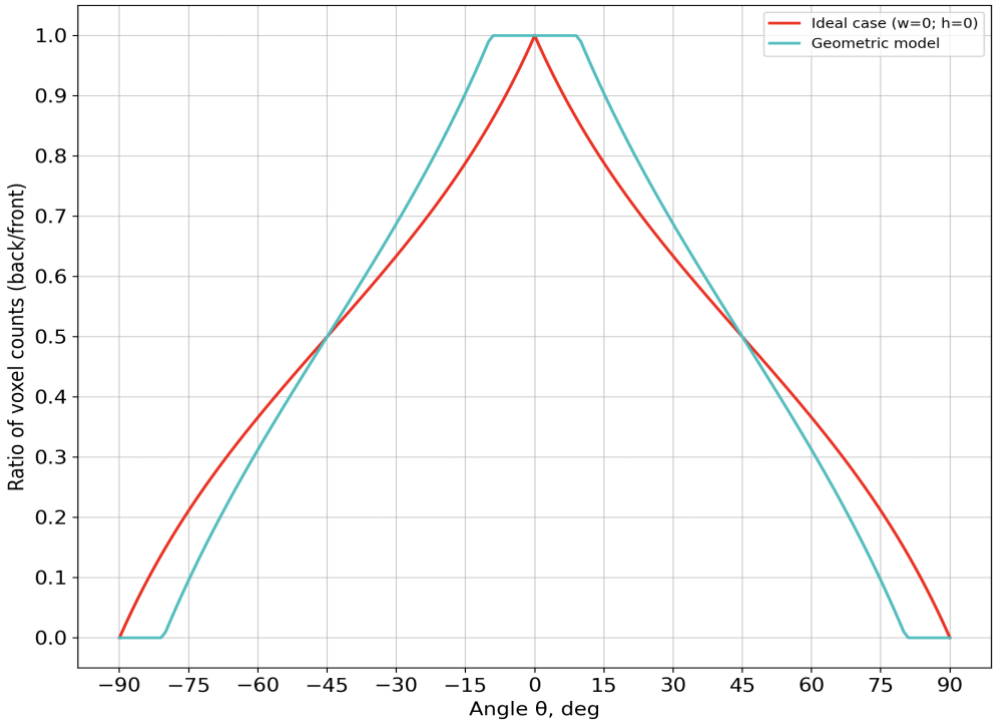

Figure 2.4. Directional capability of a 2x1 rectangular array, as predicted by the geometrical model. A shield is installed between the detectors to prevent the photons penetrating through the front detector. Parameters of the geometric model: a = 10 mm, b = 10 mm, w = 2 mm and h = 2 mm.

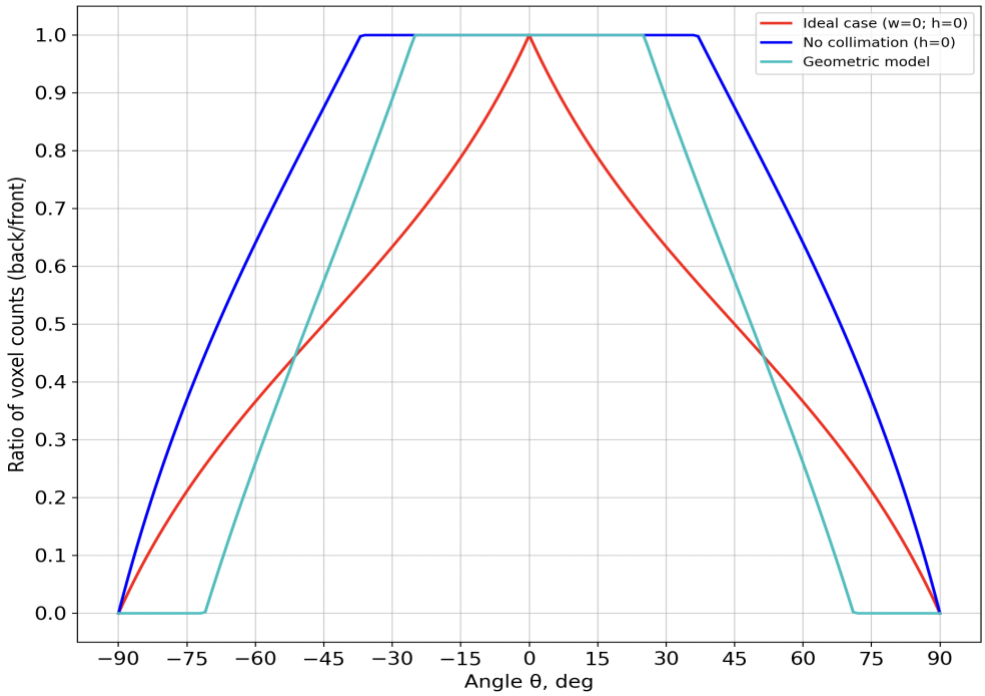

Figure 2.5. Directional capability of a 2x1 rectangular array, as predicted by the geometrical model. A shield is installed between the detectors to prevent the photons penetrating through the front detector. Parameters of the geometric model: a = 10 mm, b = 10 mm, w = 7.5 mm and h = 6 mm. These dimensions are typical of an array built from Kromek CdZnTe detectors.

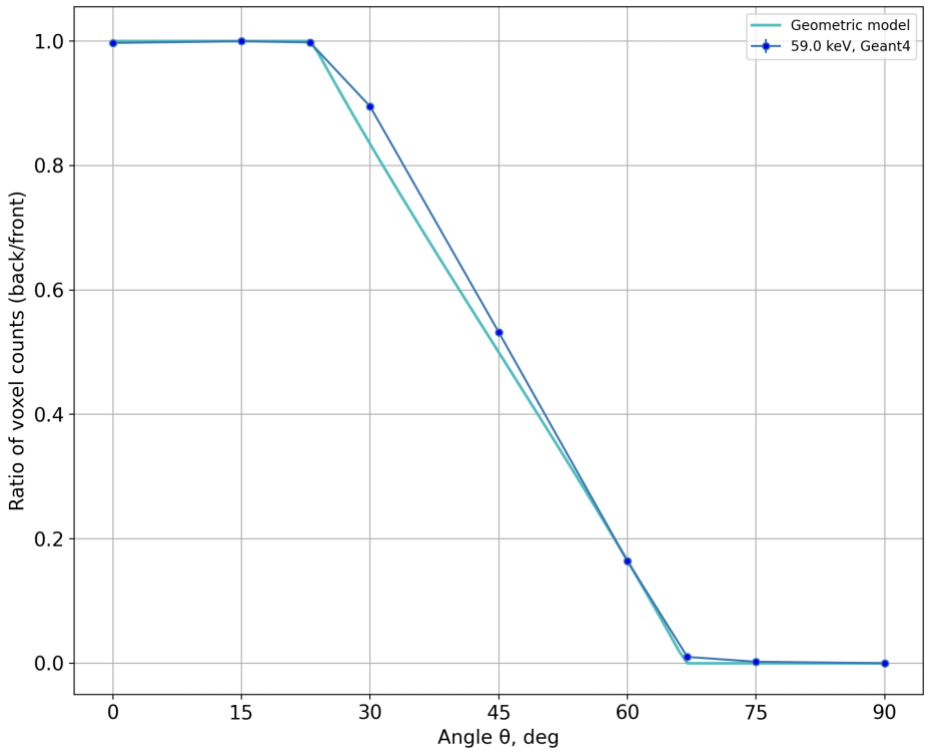

Figure 2.6. Comparison between the geometric model and Geant4 simulations for photons with an energy of 59 keV. Parameters: a = 10 mm, b = 10 mm, w = 7.5 mm and h = 7.5 mm and the width of the tungsten shield is 10 mm (Geant4).

Cylindrical detectors are widely used in various applications and these detectors can also be used for directional studies. The response model can be built by calculating the ratio of the cross-sectional areas of the back and front detectors relative to the photon beam. The back detector area is proportional to the length *XY* (Figure 2.7) whereas the front detector is always fully exposed to the beam; its cross-section is constant and proportional to the diameter of the detector (2r). Therefore, the model takes the form of:

$$R = \frac{1}{2}\left[1 + \left(1 + \frac{w}{r}\right)\sin(\alpha) - \left(1 + \frac{h}{r}\right)\cos(\alpha)\right]$$

[11]

The validity of this aquation has similar constraints as shown in Equations (1) – (4) for the rectangular model; the parameters *a* and *b* are replaced with the radius *r*.

The directional angle α must be calculated numerically. However, the response is very linear (Figure 2.8) and therefore a simple interpolation between a simulated or measured calibration curve is a more straightforward method. Here too, as in the rectangular geometry, a more practical directional angle is θ, the complementary angle of α. Figure 9 is a comparison between the geometry model and Geant4 simulations at the photon energy of 60 keV.

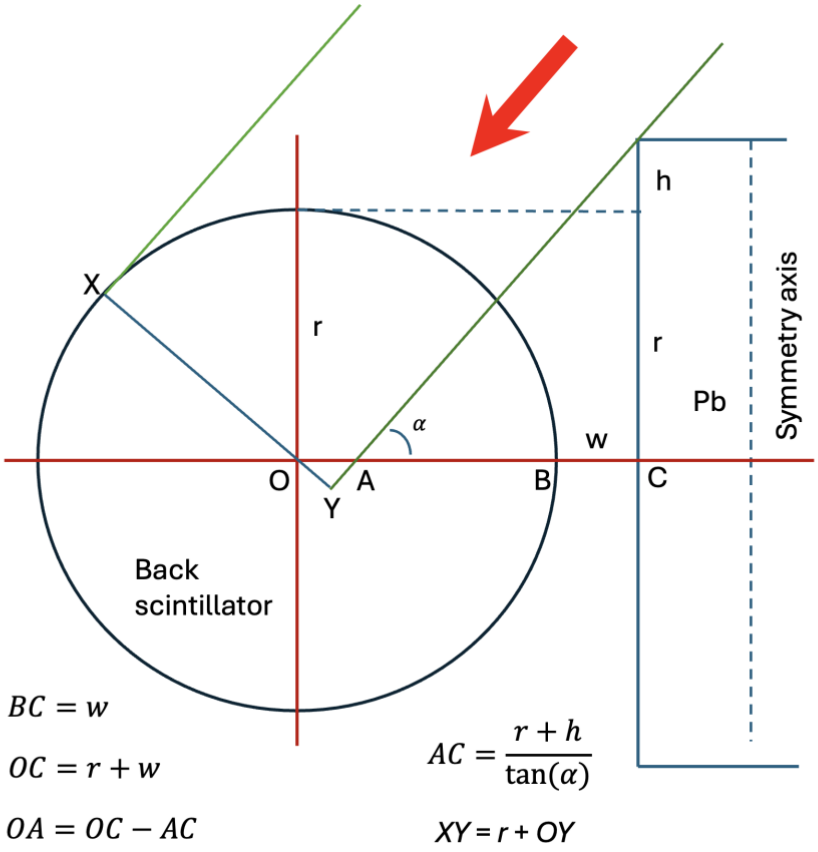

Figure 2.7. Measurement geometry for a 2x1 cylindrical array. There is a space or gap w between the back detector and the shield (front detector not drawn). The source is far away from the array (> 5 m) providing a parallel beam of photons towards the array.

The directional angle α must be calculated numerically from the Equation (11). However, the response is very linear (Figure 2.8) and therefore a simple interpolation between a simulated or measured calibration curve is a more straightforward method. Here too, as in the rectangular geometry, a more practical directional angle is θ, the complementary angle of α. Figure 2.9 is a comparison between the geometry model and Geant4 simulations at the photon energy of 60 keV.

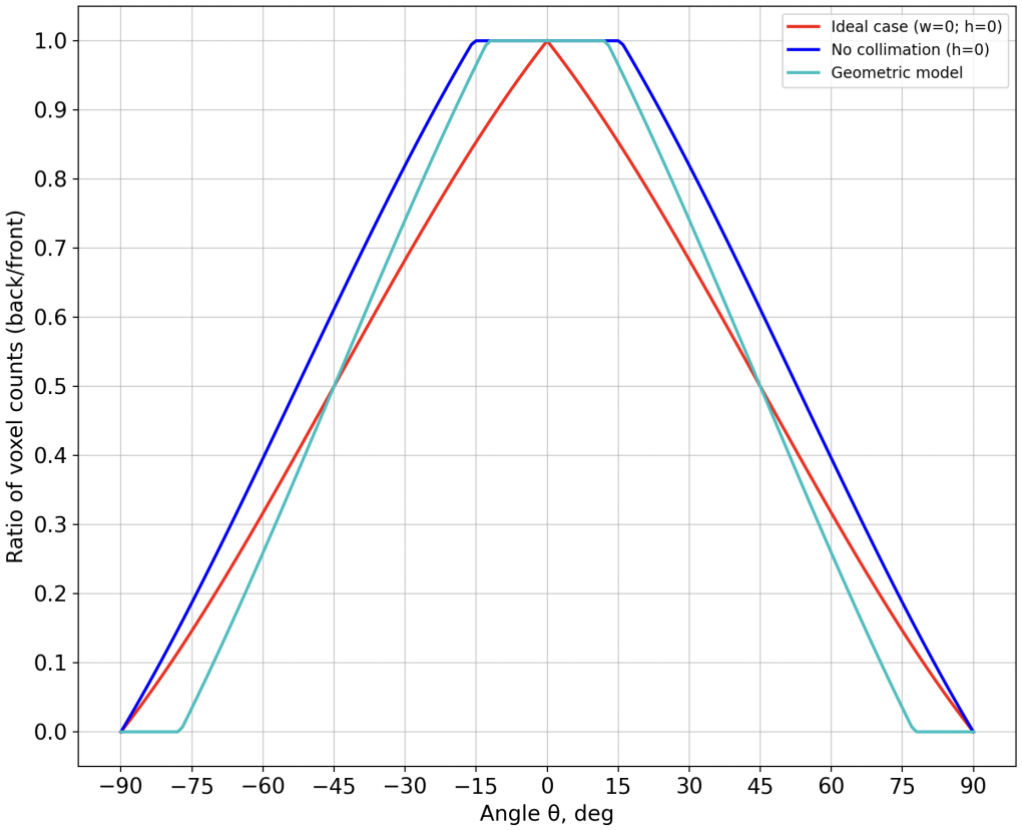

Figure 2.8. Directional capability of a 2x1 cylindrical array, as predicted by the geometrical model. A shield is installed between the detectors to prevent photons penetrating through the front detector. Parameters of the geometric model: r = 3.8 cm, w = 1.2 cm, h = 1.2 cm.

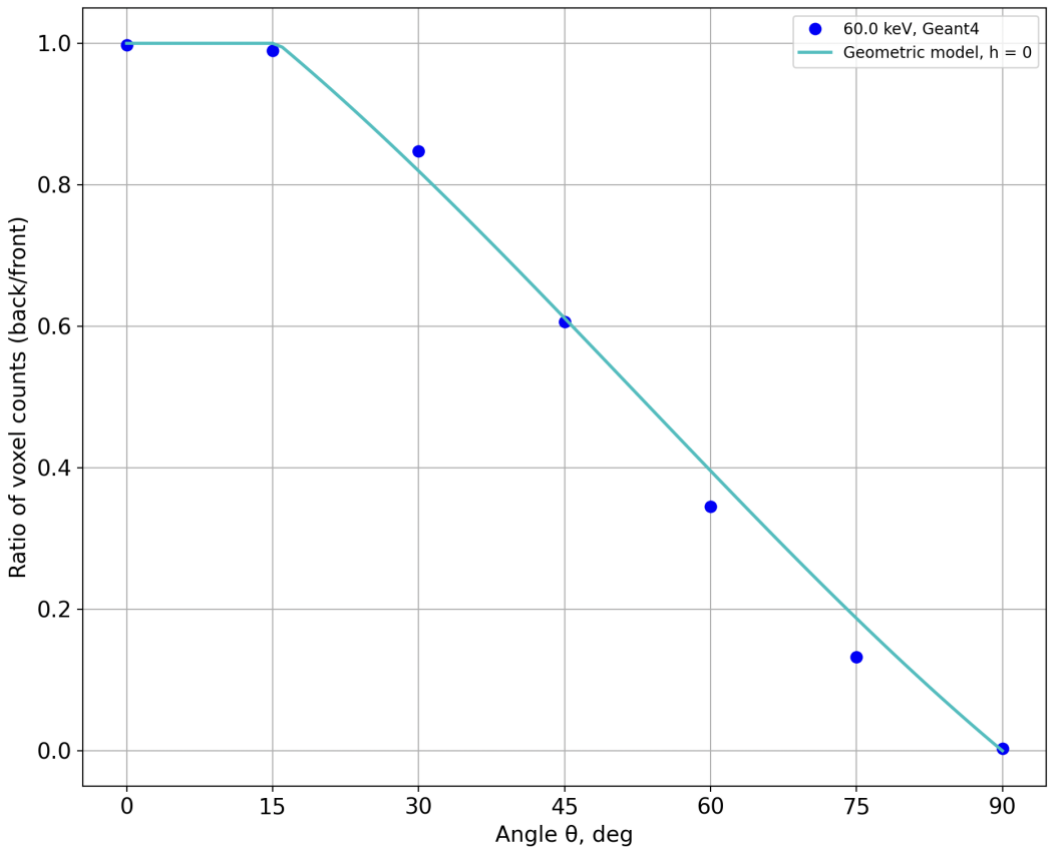

Figure 2.9. Directional capability of a 2x1 cylindrical array. Parameters of the geometric model: r = 3.8 cm, w = 1.2 cm, h = 0 cm. The data points refer to Geant4 simulations.

3. Monte Carlo analysis

In advance of the measurement campaign, the general validity of each detector setup and optimisation of model parameters were confirmed using Monte Carlo simulations. All simulations were performed in a spherical world where the lower half was comprised of concrete and the upper half of a standard air composition. All arrays were positioned on a plane 1 m above the interface of the two spheres and points sources were positioned at various distances from the simulated arrays. Point sources were monoenergetic emitters of the chosen photon energy. All simulations were conducted in Geant4 (Agostinelli et al., 2003).

4. Measurements

The measurement campaign was conducted at the facilities of the Radiation and Nuclear Safety Authority in Finland. Three primary sources were used for investigations:
Am-241 183 MBq, Cs-137 167.7 MBq and Co-60 77 MBq. Depending on the detector array used, distances between sources and the arrays were between 5 m and 1 m.

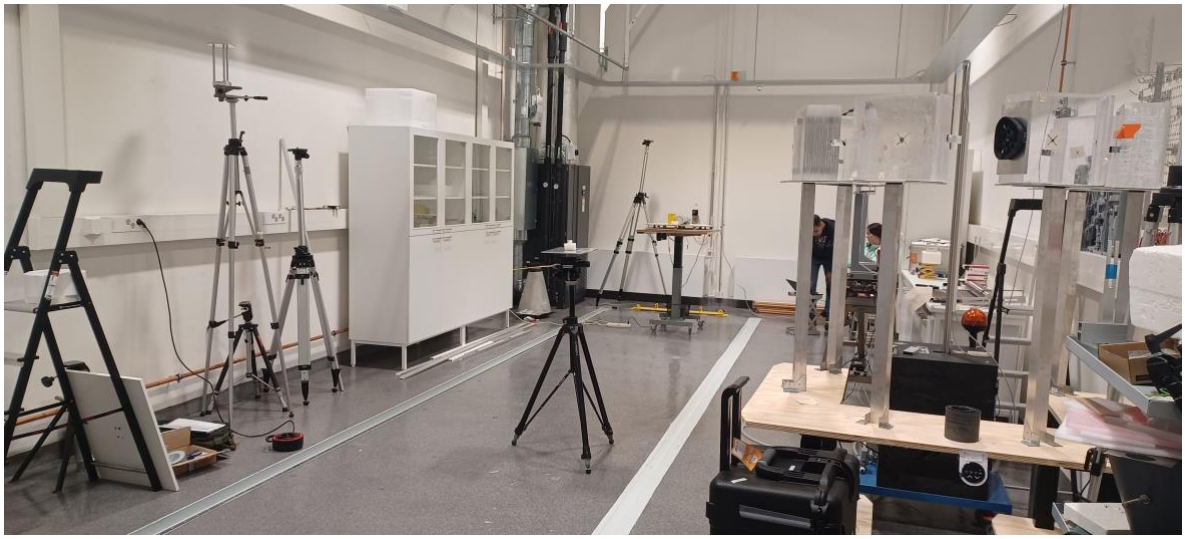

Figure 4.1. Measurement facility at STUK for directional estimation.

5. 2 x 1 Array of CdZnTe Detectors

Two 1 cm^3 CdZnTe detectors were placed in a 2 x 1 array with a 1 cm thick lead shield placed between them such that the lead shield was flush with the detector housings on all faces as depicted in Figure 5.1. For the purposes of SAMLOC, the detectors were arranged such that the source was oriented towards the mid-point of one detector and then the array was rotated in increments of 7.5 degrees relative to the source. Based on the manufacturer's specifications and scanning of the array, the two model parameters were determined to be w = 7.7 mm and h = 5.5 mm.

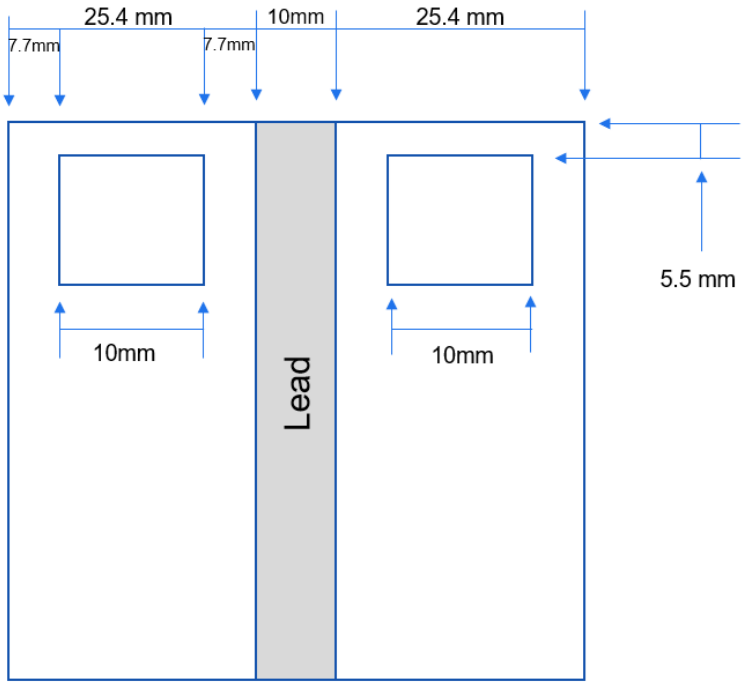

Figure 5.1. Schematic of the two CdZnTe detectors and the lead shield.

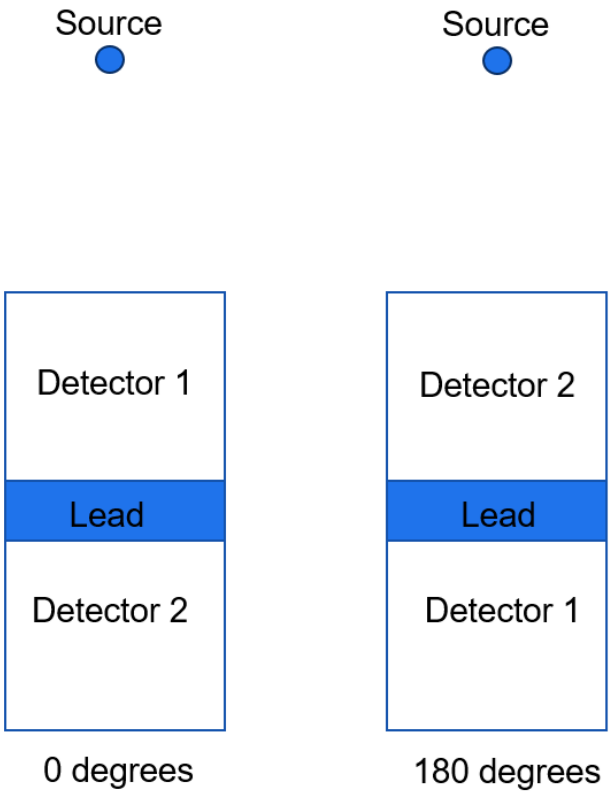

Figure 5.2. Rotation of the array relative to the source.

For the measurements, distance was measured from the centre point of the lead shield between the two detector elements and the source height was positioned at the centre line of the detector crystals. All sources were at 1 m distance. Count times varied between 300 and 800 s live time. Spectra for both detectors were recorded simultaneously at increments of 7.5 degrees between -90 and 90 degrees where 0 degrees was equal exposure for both detectors. No background correction was applied to the measurements. Count rates were determined for the 59 keV of Am-241, the 661 keV peak for Cs-137 and the 1332 keV peak for Co-60. Raw counts for each CdZnTe detector at each angle are displayed in Figures 5.3, 5.4 and 5.5 for Am-241, Cs-137 and Co-60 respectively. Ratios of count rates are displayed as a function of angle in Figures 5.6, 5.7 and 5.8.

Disparities in count rates for both detectors under conditions where equivalent count rates would have been expected (0 degrees) were observed for all three setups, indicating either a difference in efficiency for the two detectors or an error in positioning of the source relative to the array. As the difference is observed across all three setups, the latter may be less likely as an explanation. Scanning of the crystals indicated no obvious anomalies in either the crystal sizes or their positioning within the housings.

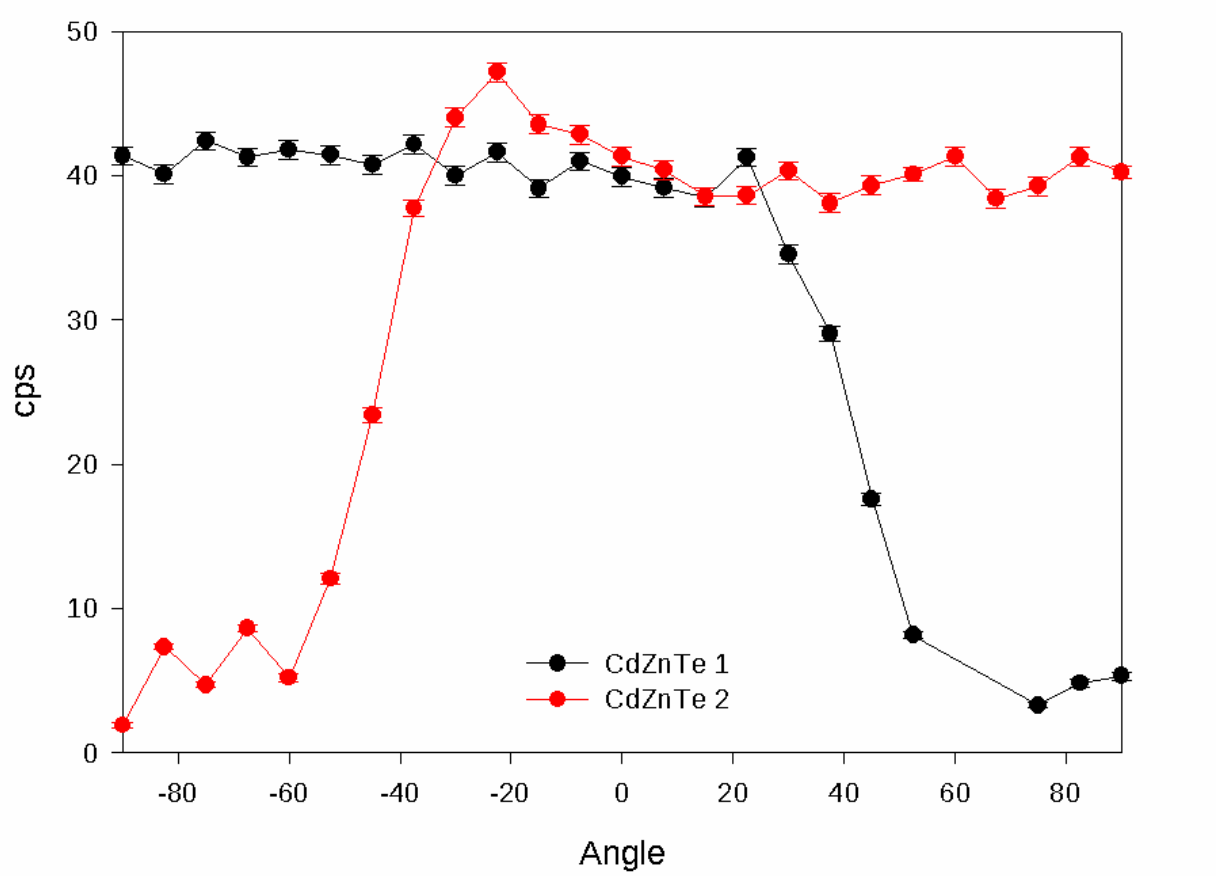

Figure 5.3. Count rates for Am-241 as a function of angle for both CdZnTe detectors.

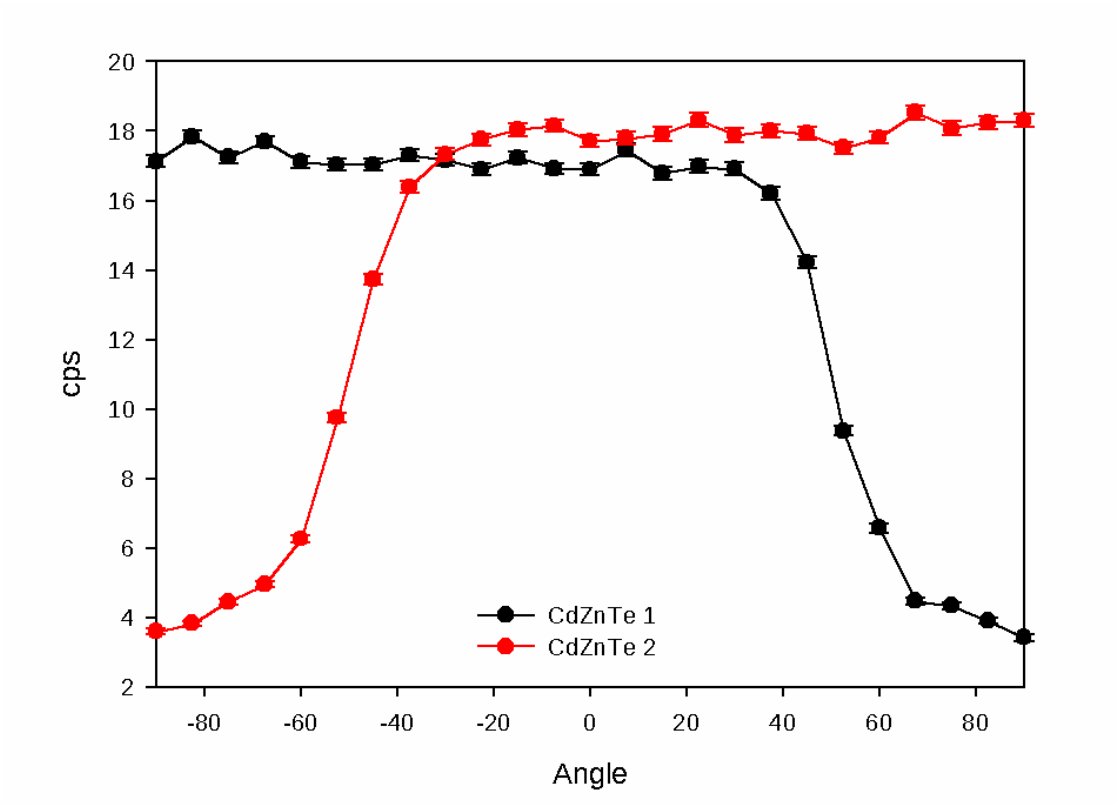

Figure 5.4. Count rates for Cs-137 as a function of angle for both CdZnTe detectors.

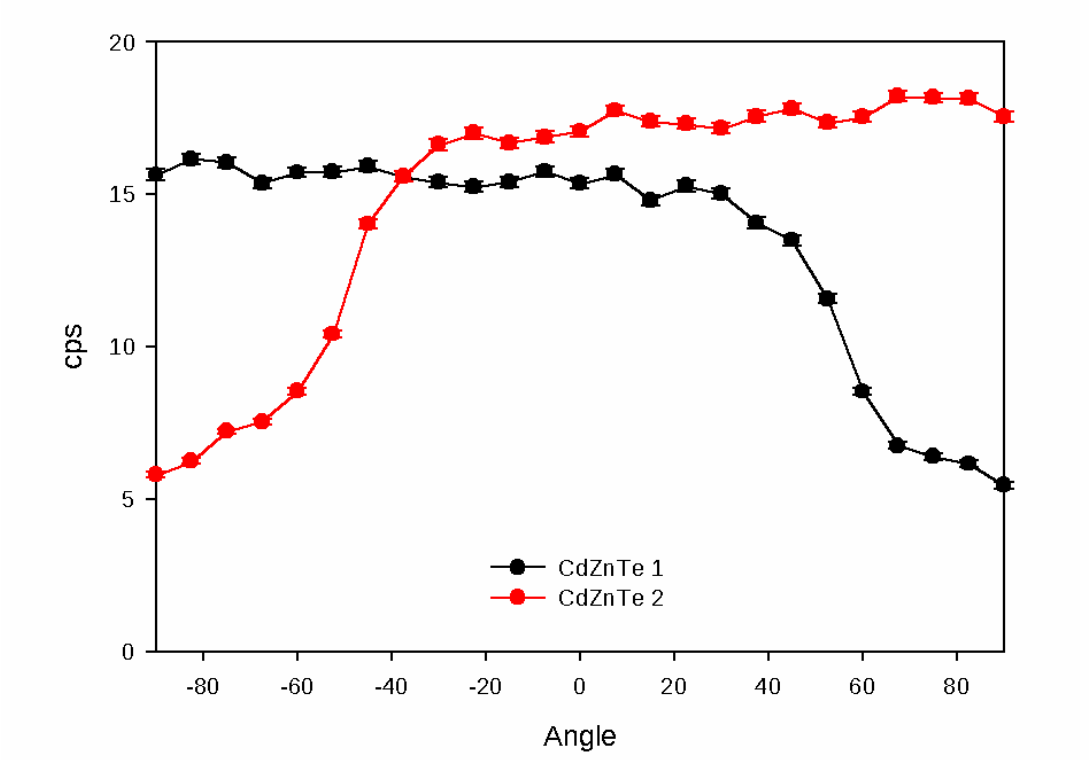

Figure 5.5. Count rates for Co-60 as a function of angle for both CdZnTe detectors.

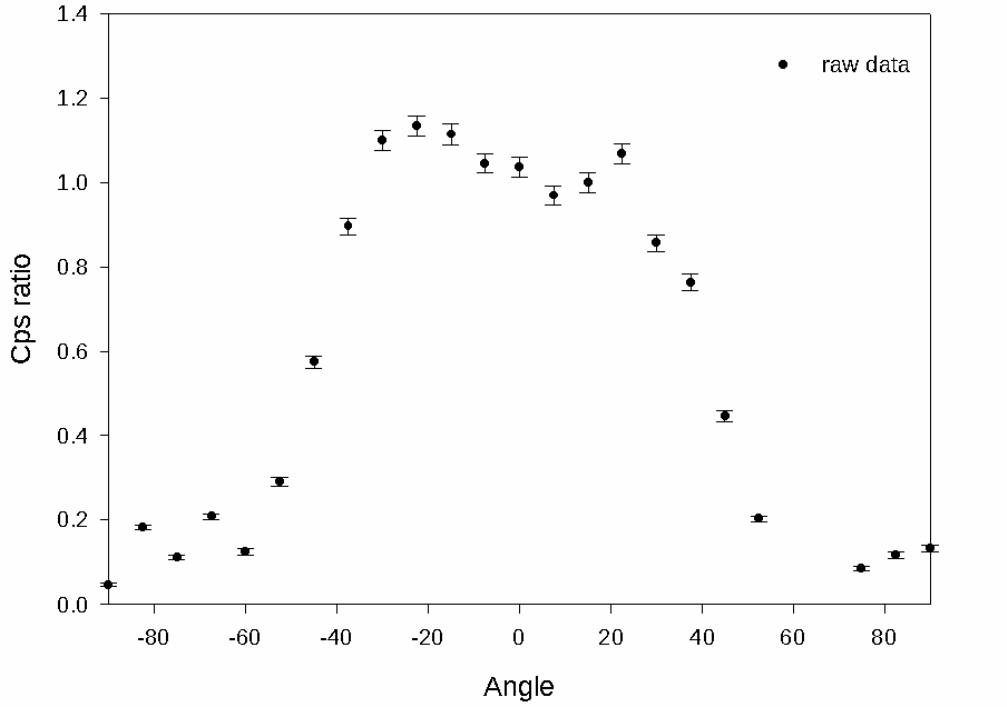

Figure 5.6. Count rate ratios for Am-241 as a function of angle for the CdZnTe detectors.

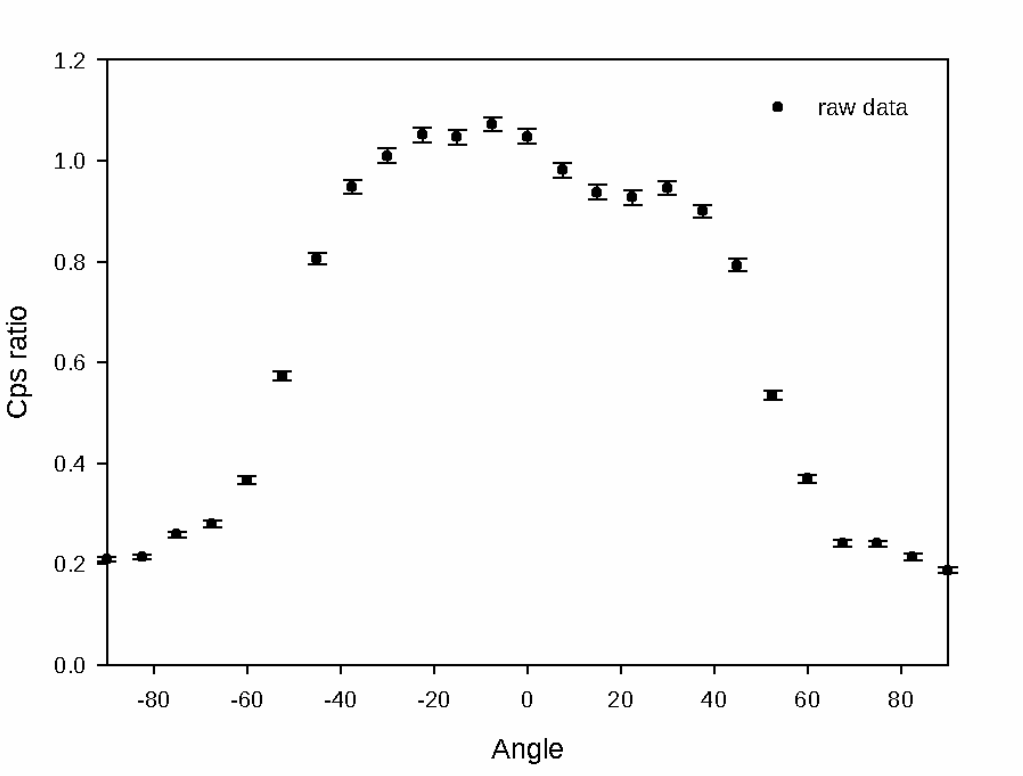

Figure 5.7. Count rate ratios for Cs-137 as a function of angle for the CdZnTe detectors.

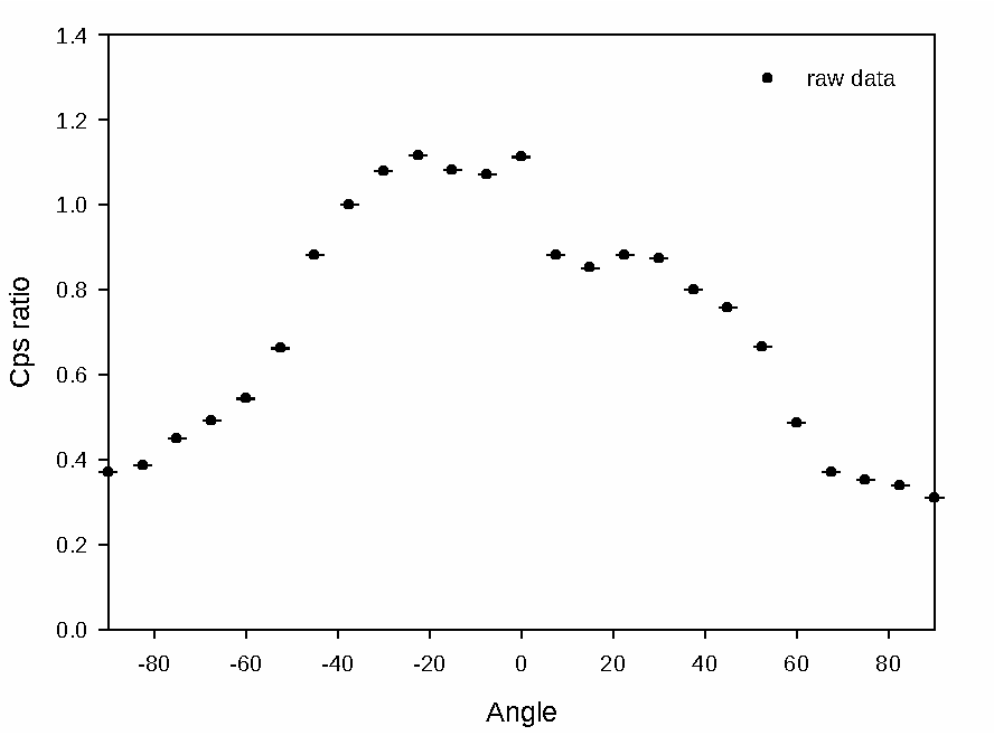

Figure 5.8. Count rate ratios for Co-60 as a function of angle for the CdZnTe detectors.

6. Array of 1.5” NaI Detectors

The source localisation measurements were performed with two different detectors. Detector *4xNaI* consisted of four cylindrical NaI(Tl) scintillators, each with a diameter of 38 mm and a length of 76 mm. The detector geometry is presented in Figure 6.1. The detector performance and the analyses algorithm used to calculate the source direction has been published in Toivonen at al., 2024; 2023.

Detector *2xNaI* consisted of two NaI(Tl) scintillators attached to a lead brick. The scintillators used were the same as in 4xNaI. The dimensions of the lead brick were 126 mm x 77 mm x 40 mm. A Co-60 gamma ray transmission image of the detector is presented in Figure 6.2. The Am-241 source was measured at a distance of 5 m, whereas the Co-60 source was measured at a distance of 10 m.

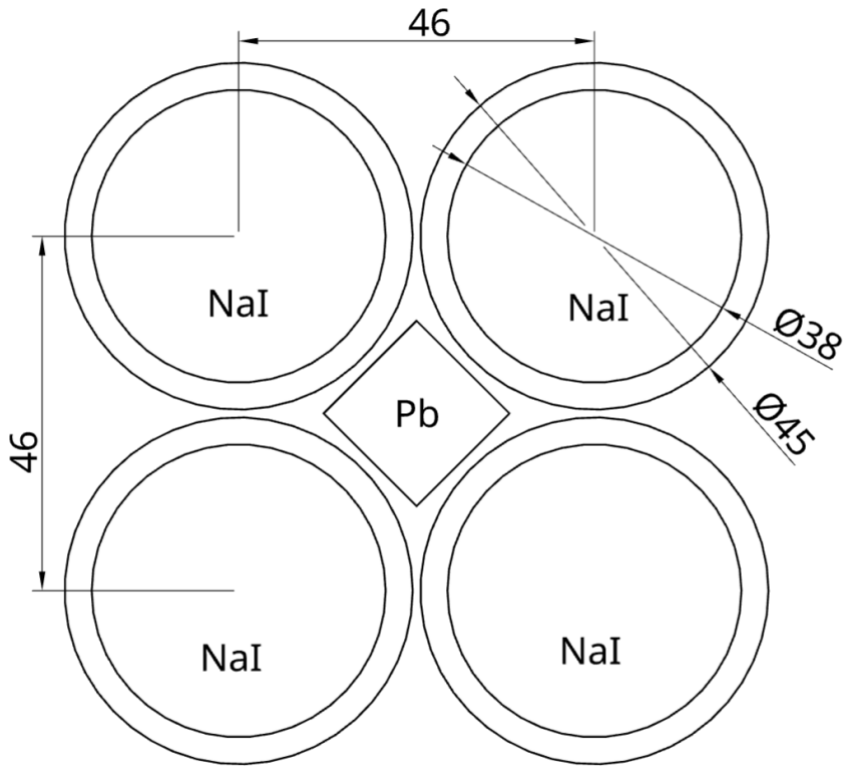

Figure 6.1. Schematic of the *4xNaI* detector geometry.

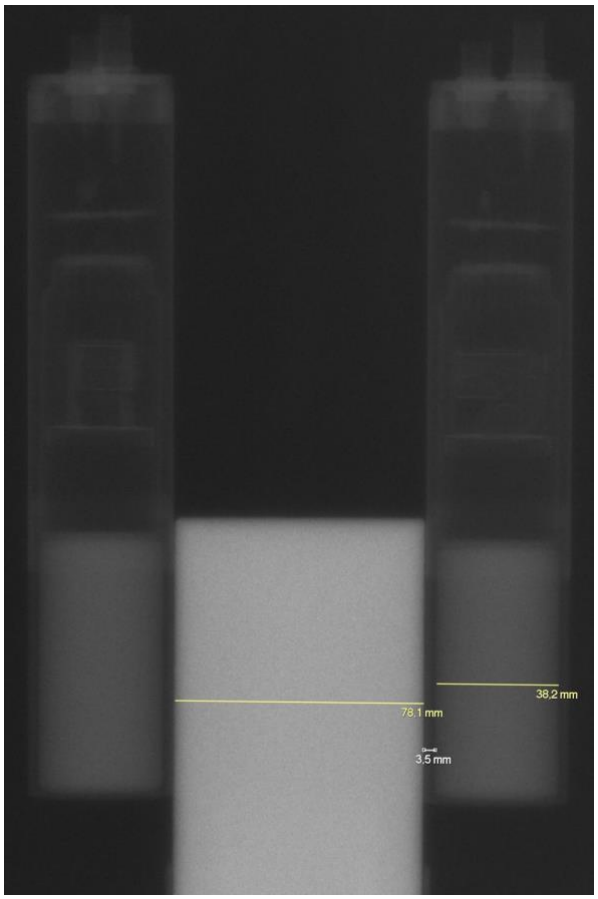

Figure 6.2. Co-60 gamma ray transmission image of the *2xNaI* detector.

Summary of the uncertainties of the calculated source directions in all measurements is presented in Table 1.

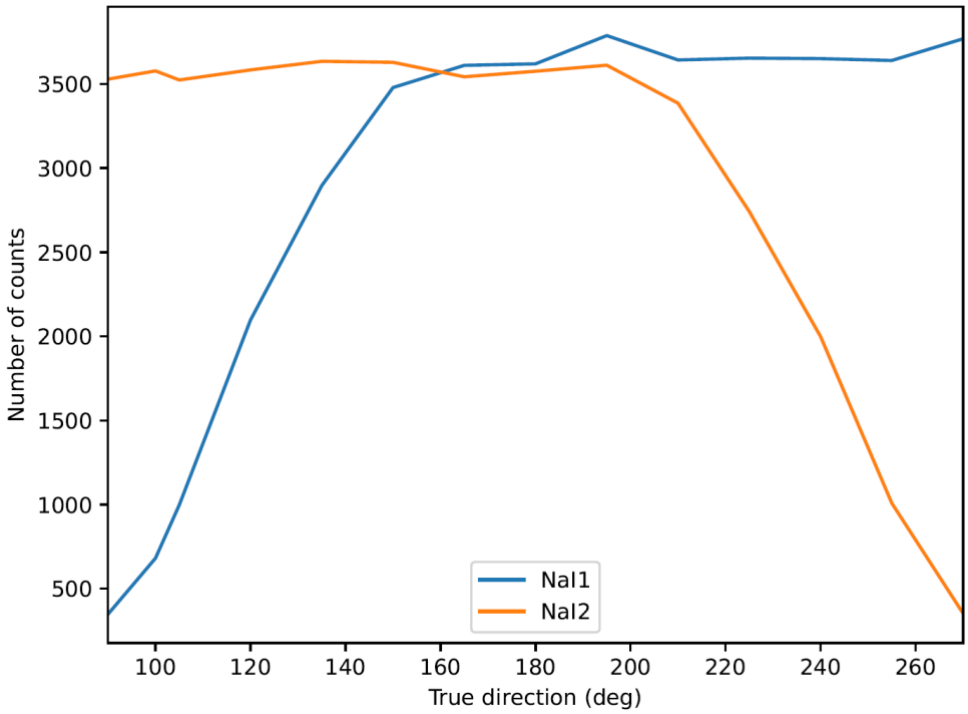

Figure 6.3. Number of counts recorded in the Co-60 measurements in 100 s with the *2xNaI* detector. Please note: 90 deg and 270 deg in the above figure are equivalent to the -90 +90 notation as used in previous figures.

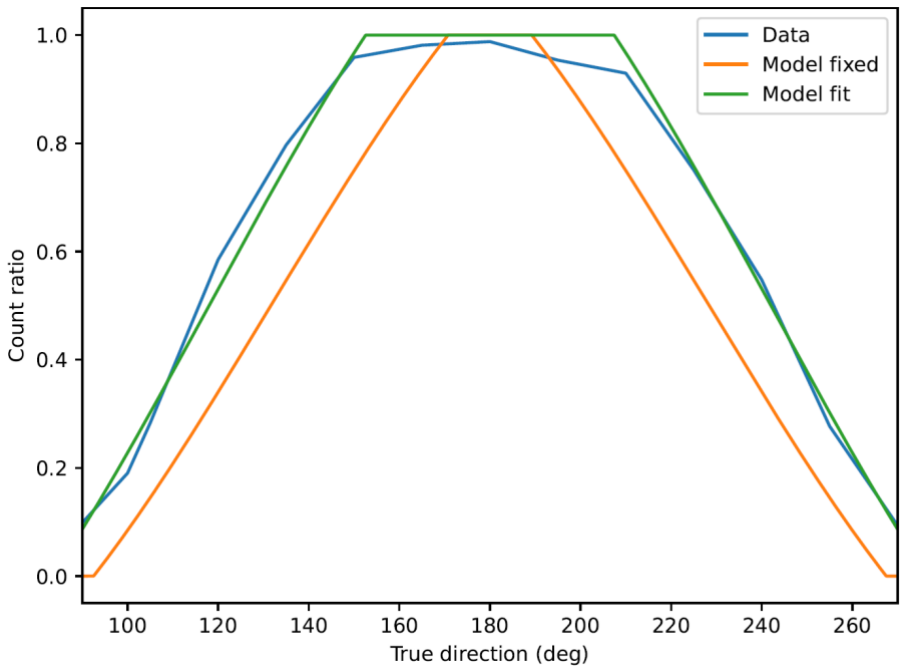

Figure 6.4. Ratio of the count rates of the two scintillators in the *2xNaI* detector. Data - data measured from the Co-60 source. Model fixed - theoretical model obtained by using measured detector geometry. Model fit - theoretical model fitted to the measured data by keeping the absorber width and the gap between the crystal and the absorber as free parameters. Please note: 90 deg and 270 deg in the above figure are equivalent to the -90 +90 notation as used in previous figures.

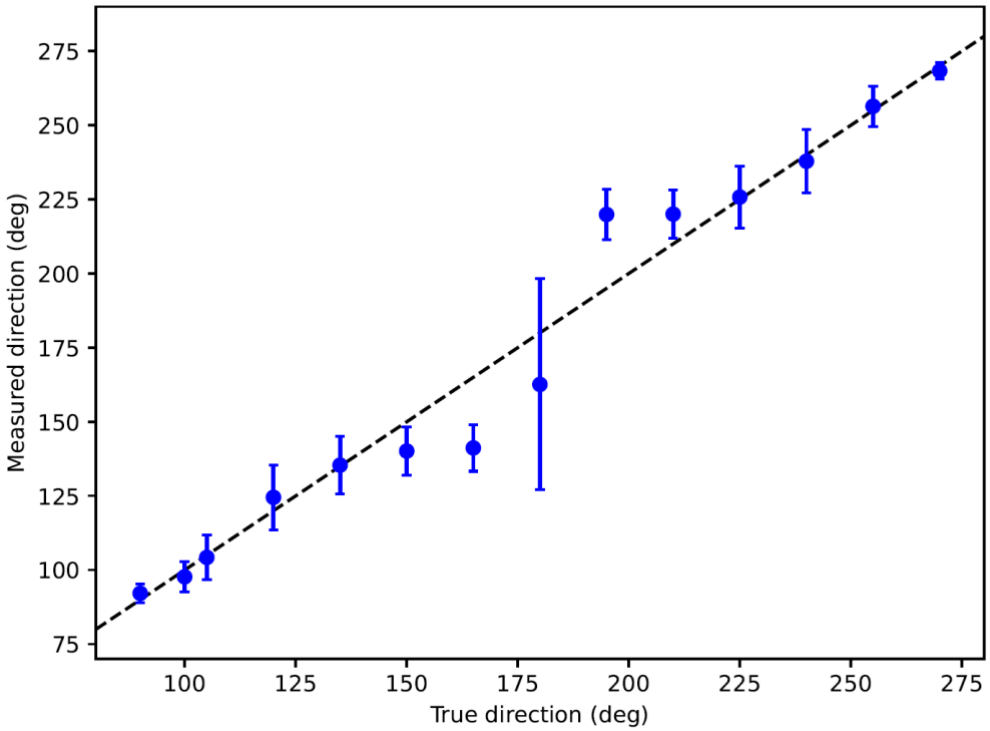

Figure 6.5. Co-60 source direction estimated from the data recorded with the *2xNaI* detector. The error bars represent the standard deviation of the estimated uncertainties in 1 s measurements. Please note: 90 deg and 270 deg in the above figure are equivalent to the -90 +90 notation as used in previous figures.

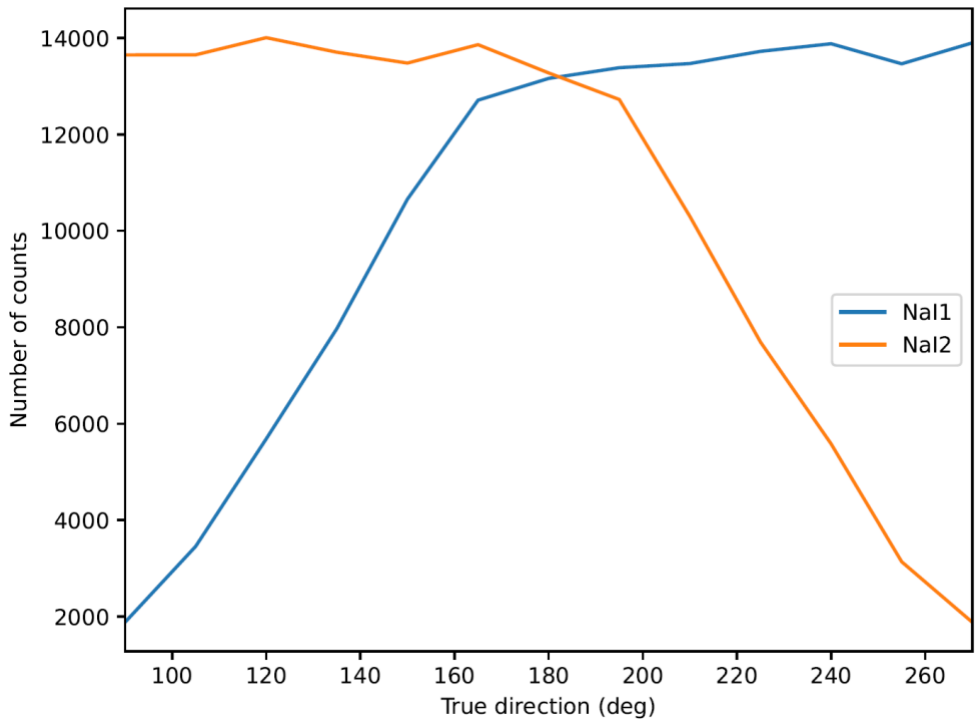

Figure 6.6. Number of counts recorded in the Am-241 measurements in 100 s with the *2xNaI* detector. Please note: 90 deg and 270 deg in the above figure are equivalent to the -90 +90 notation as used in previous figures.

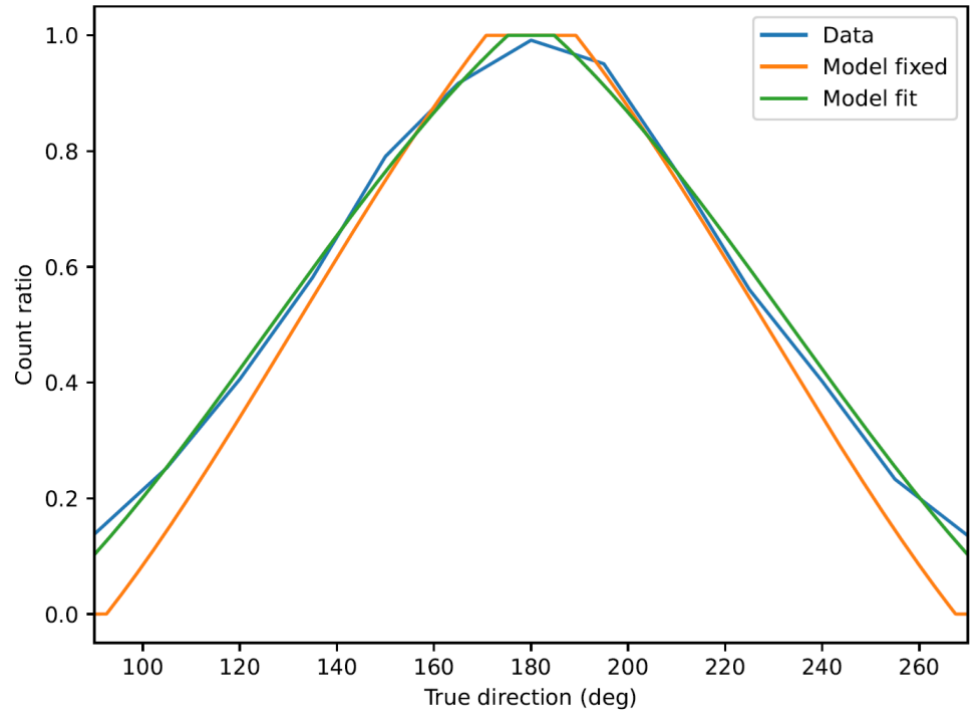

Figure 6.7. Ratio of the count rates of the two scintillators in the 2xNaI detector. Data - data measured from the Am-241 source. Model fixed - theoretical model obtained by using measured detector geometry. Model fit - theoretical model fitted to the measured data by keeping the absorber width and the gap between the crystal and the absorber as free parameters. Please note: 90 deg and 270 deg in the above figure are equivalent to the -90 +90 notation as used in previous figures.

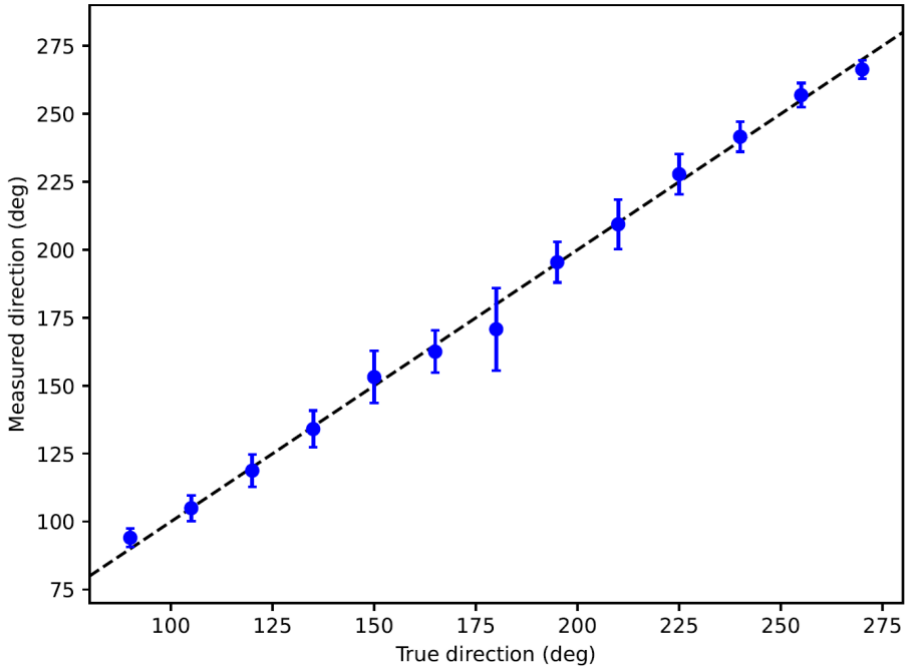

Figure 6.8. Am-241 source direction estimated from the data recorded with the *2xNaI* detector. The error bars represent the standard deviation of the estimated uncertainties in 1 s measurements. Please note: 90 deg and 270 deg in the above figure are equivalent to the -90 +90 notation as used in previous figures.

Isotope	**Activity**	**Distance**	***2xNaI*** **Direction unc**	***4xNaI*** **Direction unc**
Cs-137	168 MBq	5 m	15.6 deg	5.4 deg
Co-60	77 MBq	10 m	16.6 deg	9.1 deg
Am-241	183 MBq	5 m	8.3 deg	5.1 deg

Table 1. Standard uncertainty of the calculated source direction in 1 s measurements.

Based on this study, information on the source direction can be obtained by using a detector consisting of only two scintillator elements. However, a detector with four scintillator elements has a clear edge on direction measurements for five reasons:

- With two elements, two source directions give exactly the same signal. In the worst case, these directions differ 180 degrees from each other. With four elements, the signal response for each angle is unique.
- With two elements, the accuracy of the measured direction depends strongly on the angle of the source. The accuracy is especially poor close to the angles 0 and 180 degrees where both detector elements have identical efficiency. With four detector elements, the direction accuracy is almost independent of the source direction.
- With two elements, the analysis algorithm only works reasonably if the geometry parameters are fitted to the measured data. The fitted parameters also depend on the source energy. With four detector elements, model parameter fitting is not required, and the model used is independent of the source energy.

- The direction analysis model for the detector with two elements only works for fitted peak areas or a narrow region of interest around the photo peak. Thus, the direction calculation requires peak identification. With four elements, the source direction can be calculated from the total number of counts in the spectrum.
- On average, a detector with four elements has higher direction accuracy than a detector with two elements.

7. Array of Two 1 l NaI Detectors

This array consisted of two 1 l detectors with dimensions of 5 x 10 x 20 cm placed on either side of 4 cm of lead shielding as depicted in Figure 7.1. The parameters for the model were as follows: a = 5 cm, b = 10 cm, w = 5.5 cm, h = 2 + 4 cm = 6 cm. The geometry of the detectors may not be ideal for the experiments, due to the relatively large gap between the crystal and the detector housing, resulting in an equally large gap between the crystal and the lead. This has the effect of the insensitive angle around 180° being much larger than if the gap could be minimized. Despite this drawback the results are promising. Measurements were done for Am-241 in the angle range 0 to 180°, for Cs-137 in the angle range -90 to +90°, and for Co-60 in the angle range -90 to +90°. For Am-241 the distance from detector to source was 2.21 m, for Cs-137 measurements were done at distances of 5 m and 10 m, and for Co-60 the measurements were done at a distance of 10 m.

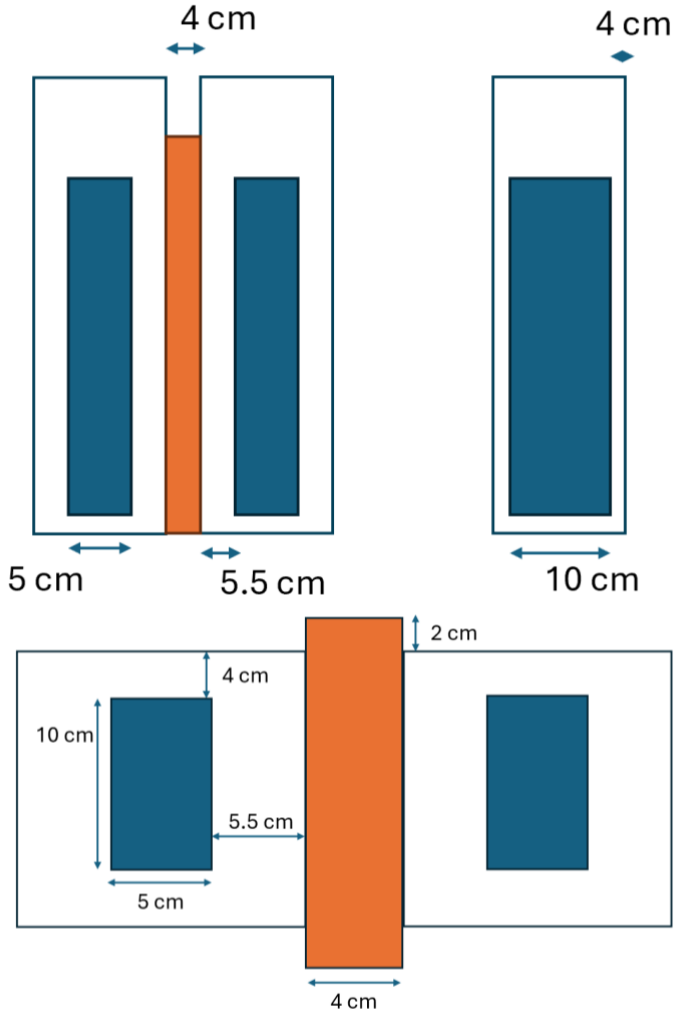

Figure 7.1. Arrangement of the 2 x 2 l NaI array with associated lead shielding. Top – side view, bottom – view from above.

For Am-241, the measurements were performed at a distance of 2.21 m, from 0 to 180°, at 10° intervals. The ratio of the 59.6 keV peak areas (back detector/front detector), normalized to the ratio at 0° is plotted against angle in Figure 7.2. It is evident that the insensitive angle, where the ratio between the peaks is close to 1, is quite large, spanning some 30° either side of 0. Furthermore, the peak ratio is very close to 0 for a large area around the 90° angle, some 20 degrees on each side. This is caused by a) the geometry of the detector setup allowing the back detector to be effectively shielded even at 10 and 20°, and b) the low energy of the Am-241 photons not being able to penetrate through the shielding. There is not very good agreement between the experimental results for Am-241 and the geometric model in the angle range where it should give us a good indication of direction to the source, with the difference between the experimental results and the model predictions ranging from 5 to 40°. This may be explained the Am-241 photons being very efficiently shielded and scattered by the detectors and perhaps even the detector housing, due to their low energy.

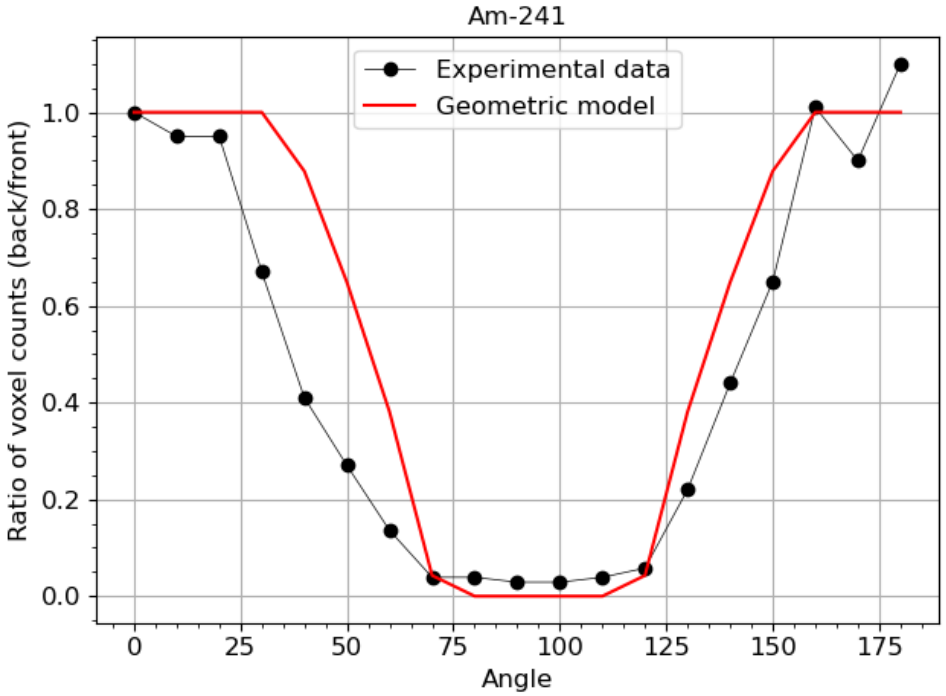

Figure 7.2. Ratio of the 59.6 keV peak areas (back detector/front detector), normalized to the ratio at 0°.Experimental data is plotted in black and the geometric model is plotted in red.

Two data sets were obtained for Cs-137, one at 5 m and one at 10 m. measurements were done in 10° intervals from -90 to +90° at both distances. The ratio of the 661 keV peak areas (back detector/front detector), normalized to the ratio at 0° is plotted against angle in Figure 7.3. As with Am-241 we see a large insensitive area around 0°, of roughly 30 - 40° to either side. However, the results around 90° are much more well behaved, as the shielding is less effective for the higher energy photons. The two graphs are very similar, and the normalized peak ratios almost identical, indicating that, as expected, this analysis is not distance dependent, assuming it is close enough for good counting statistics.

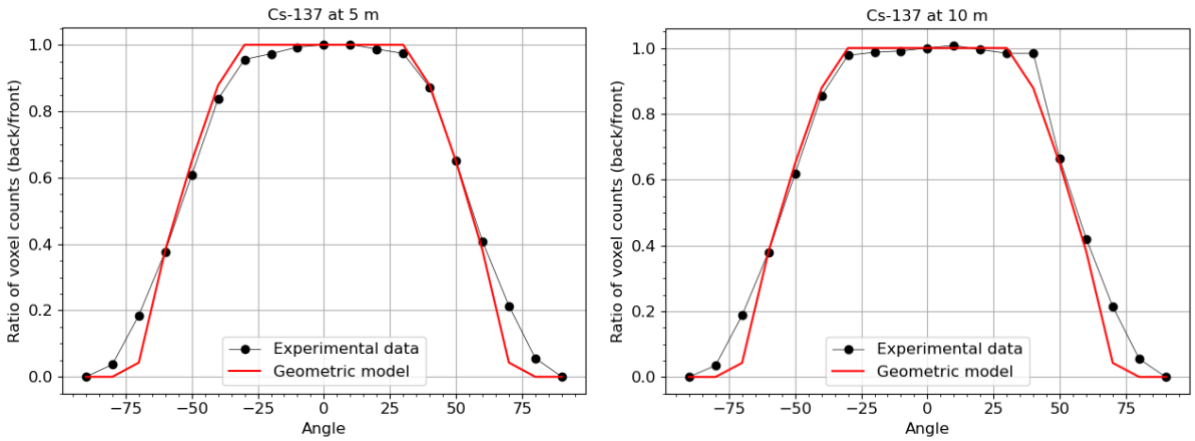

Figure 7.3. Ratio of the 661 keV peak areas (back detector/front detector), normalized to the ratio at 0° at 5 m (left) and 10 m (right) Experimental data is plotted in black and the geometric model is plotted in red.

Aside from the large insensitive angle between -30 and +30°, caused by detector geometry, there is much better agreement between the experimental data and the geometric model for Cs-137 than for Am-241. The difference between the experimental data and the model prediction is around 10° where it is largest.

Measurements of Co-60 were done at a distance of 10 m, from -90 to +90° at 10° intervals. Co-60 has two peaks in the gamma spectrum, at 1173 keV and 1332 keV respectively. The peak analysis was carried out for both peaks separately and an average of the normalized ratio between the two peaks was also calculated.

As for both Am-241 and Cs-137 the insensitive area around 0° is quite large, spanning 30-40° in either direction. The behaviour around 90° is similar to the results of Cs-137, with the difference that not all the high energy gamma photons from Co-60 are stopped by the lead, resulting in the peak ratio at 90° being above 0, in contrast to the same angle for Cs-137. The agreement between experimental data and the geometric model is quite good, with the difference, where it is largest, being around 10-15°.

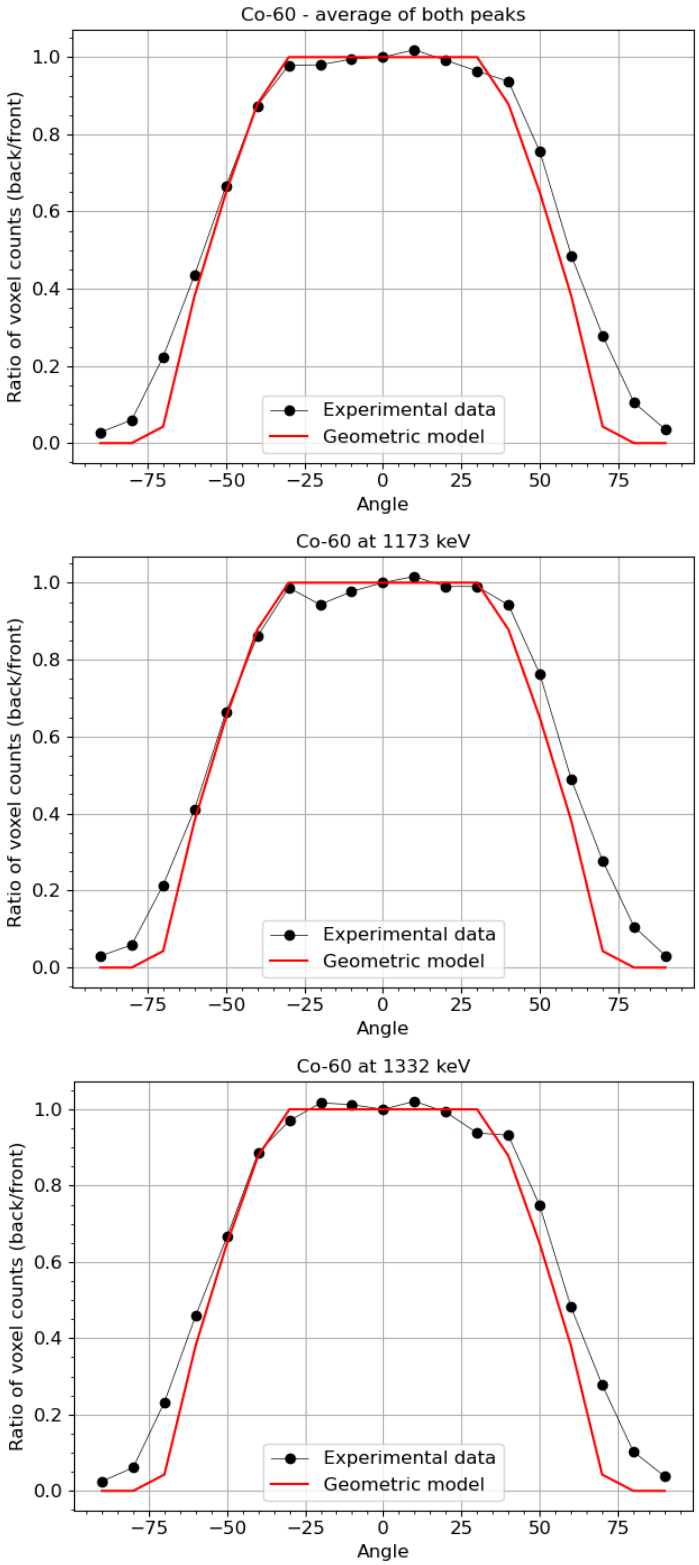

Figure 7.4. Ratio of the average of the two Co-60 peak areas (back detector/front detector), normalized to the ratio at 0° at 10 m (top) and for the individual peaks (middle and bottom).The experimental data is plotted in black and the geometric model is plotted in red.

8. Utilisation of One 3” NaI Detector

The source direction-localisation experiments were carried out at STUK’s (Radiation and Nuclear Safety Authority of Finland) irradiation facility on 23-26 September 2024. A 3"x3" NaI(Tl) detector from Ortec was used. The detector's housing was made by aluminium in a cylindrical shape with dimensions of 100 mm (outer diameter), 5 mm material thickness, and the detector's front plate was 2 mm thick. The scintillation crystal's front surface was 27 mm from the outside of the aluminium front plate.

A single detector was used with the lead shield. A one-detector geometry with a shield on the side may be used as an alternative of using two detectors with an intermediate shield. However, two measurements for each direction of the radiation source are required, with the shield on either side of the detector. The thickness of the lead shield was 8 cm, which makes the absence of a second detector with its small additional shielding effect negligible. With this technique, it is possible to eliminate discrepancies arising from intrinsic differences between two detectors. The detector-shield set-up was positioned on a wooden rotating plate. This allowed the whole set-up to obtain irradiations at any angle to the radiation source. Measurements were acquired in 10-degree intervals, from the irradiation of the detector straight towards the source (0 degrees) to the side (90 degrees).

The distance between the detector's front surface and the sources was approximately 4.8 m. The detector was positioned in such way that the centre of the NaI(Tl) crystal was located at the centre of the turntable. For the Am-241 measurements, one setup was used, with the lead shielding aligned to the front surface of the detector housing (top Figure 8.1). For the Cs-137 measurements, two setups were applied (Figure 8.1), with the lead shielding aligned to the front of the scintillation crystal and to the front surface of the detector housing, as for the Am-241 measurement.

To avoid energy drift during the measurements, the maximum count rate in channel 500 (corresponding to the K-40 photopeak) was controlled between each measurement. A shift of the energy peak by one channel (either to the left or to the right) was considered insignificant.

Raw data extraction was performed semi-automatically using a Python 3.12 script (https://test.pypi.org/project/spec-reader/). Data treatment and statistical analysis were conducted using Microsoft Excel. Data were described by the range, mean, and standard deviation.

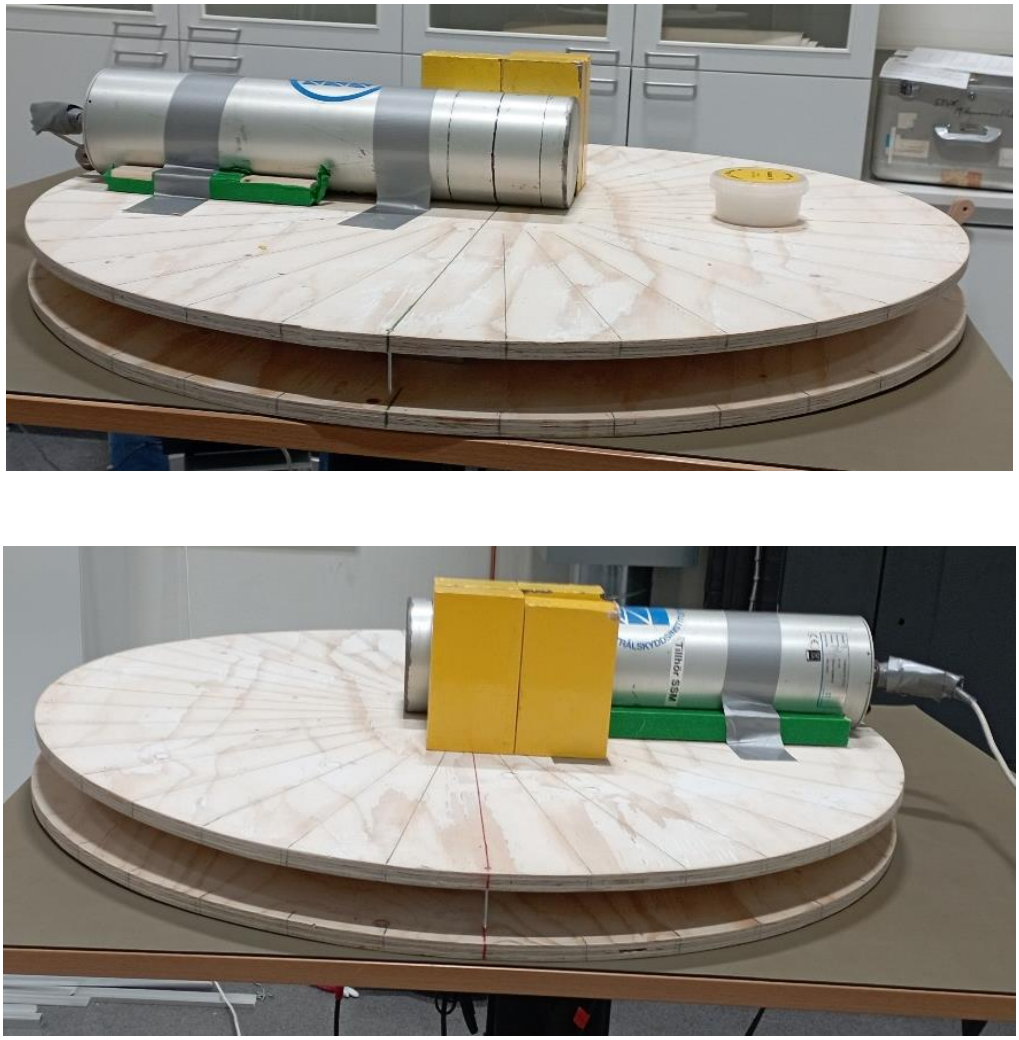

Figure 8.1. The experimental setup on the wooden circular plate, with lead shielding aligned to the edge of the detector housing (top) and to the crystal edge (bottom).

Background measurements were conducted during the first day, when no other radiation sources were present in the room. However, since the background varied among the days (mainly due to the presence of other radiation sources in adjacent irradiation halls), the calculation of the net counts was not based on the subtraction of the background as measured during the first day. Instead, we chose an implemented function of net area calculation based on Ortec´s Maestro software, which minimizes the influence of varying backgrounds.

The registered full energy peak areas correspond to the net count rate of photons from the source with the detector shielded and unshielded. The reported ratio (R) corresponds to the ratio of the shielded count rate divided by the unshielded count rate for each angle. The uncertainties (σ_R) were calculated by the uncertainty propagation method. Table 2 and Figures 8.2, 8.3 and 8.4 present all ratios for the three experimental setups, along with the final uncertainties.

	Am-241 (detector)		Cs-137 (detector)		Cs-137 (crystal)	
Angle	**R**	**σ_R**	**R**	**σ_R**	**R**	**σ_R**
0°	1.002	0.014	0.977	0.007	1.003	0.008
10°	0.959	0.012	0.999	0.008	0.994	0.008
20°	0.886	0.012	0.922	0.007	0.989	0.008
30°	0.753	0.010	0.805	0.007	0.937	0.008
40°	0.578	0.007	0.602	0.005	0.831	0.007
50°	0.385	0.005	0.353	0.004	0.645	0.006
60°	0.193	0.003	0.151	0.003	0.442	0.005
70°	0.039	0.002	0.012	0.001	0.206	0.002
80°	0.009	0.002	0.000	0.001	0.074	0.001
90°	0.000	-	0.000	0.001	0.000	0.000

Table 2. Ratio of the net area count rate of the shielded to unshielded detector for Am-241 and Cs-137 with the lead shield in different positions in relation to the detector.

Figure 8.2. Ratio of shielded to unshielded, CPS in the full energy peak of the Am-241 source, with respect to the direction between the source and detector.

Figure 8.3. Ratio of unshielded to shielded, CPS in the full energy peak of a Cs-137 source, for various angles between the source and the detector. The blue data points correspond to the alignment of the lead shield to the detector, while the orange data points refer to the alignment of the lead shield to the crystal.

Figure 8.4. Ratio of unshielded to shielded CPS with respect to the direction for Cs-137 (blue data points) and Am-241 (purple data points) measurements, when the lead shielding is aligned to the detector.

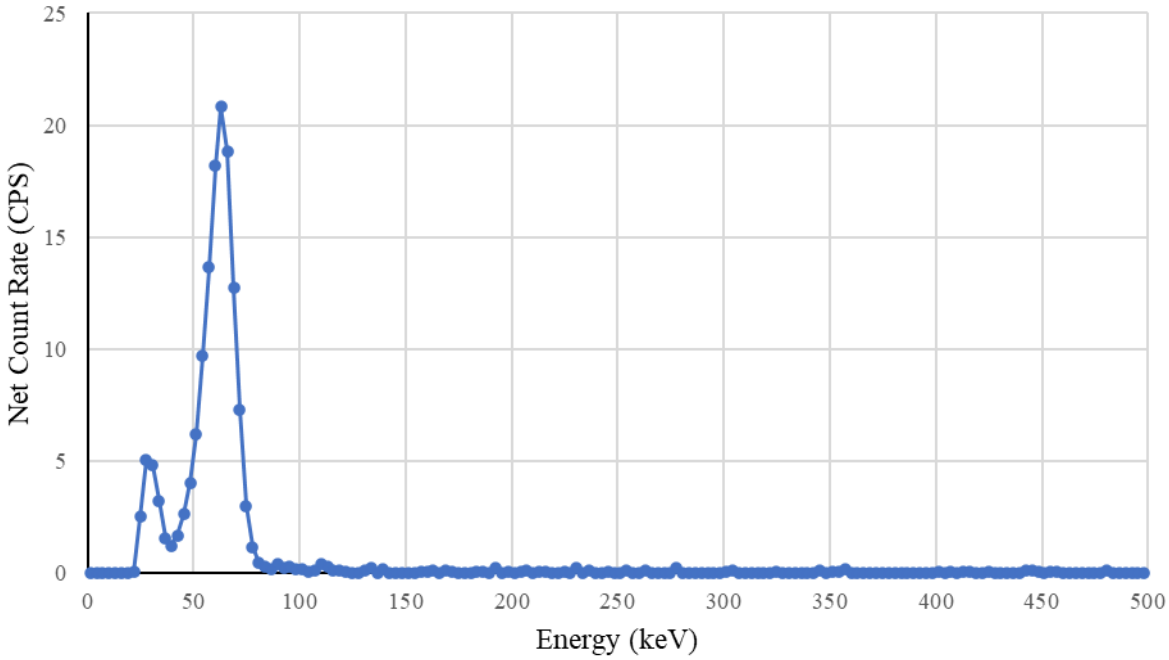

Figure 8.5. Net count rate (CPS vs energy) with manually removed background for Am-241 when the detector was fully shielded

The position of the lead shield relative to the detector crystal significantly affects the drift of count rate ratios (see Figure 8.3), which in turn impacts the accuracy of determining the azimuth of source location. When the lead shield is aligned to the crystal, the method is sensitive to changes in the angle close to 90 degrees because the lead shield affects the count rate in the full-energy peak of the shielded detector as soon as the angle decreases from 90 degrees. In other words, decreasing the angles below 90 degrees causes the photons' path length through the lead to decrease. On the other hand, if the lead shield is further forward, as when it is aligned with the detector's outer casing, then the area just below the 90-degree angle becomes insensitive to angle changes up to 70 degrees as the front of the crystal is 27 mm behind the front of the lead shield. The reversal in angular sensitivity applies to angles close to 0 degrees, as shown in Figure 8.3.

The low resolution of a NaI(Tl) crystal implies that not only primary photons contribute to registrations in the full energy peak, but also Compton scattered photons. For 662 keV primary photons from Cs-137, Compton photons with scattering angles between 0 and 25 degrees may also be registered in the full energy peak. For 59.5 keV primary photons from Am-241, Compton-scattered photons with scattering angles up to 180 degrees have energies between 48.3 and 59.5 keV, almost all that could be recorded in the region of the full energy peak.

The presence of Compton photons in the full energy peaks means that determining the angle of a photon source with two detectors and an intermediate lead shield is not as "pure" as the theory says, based solely on the absorption of primary photons in the detector. A small part of the registrations in the full energy peak is due to Compton photons from surrounding material. The method becomes somewhat dependent on material in the environment around the radiation source and the detector. Compton photons may affect the area of the full-energy peak e.g. when locating a radiation source in a packed cargo space. This effect can be seen in

Figure 8.5, where Compton photons from Am-241 were registered in the full energy peak area even though there was 8 cm of lead between the source and the detector. When calculating the ratio in the full energy peak area, the net count rate of the shielded detector was 7.8% of the net count rate observed in the unshielded detector, when calculating the net areas with manual subtraction of the background from the gross area (instead of the Maestro function).

9. Array of Two 4”x4”x16” NaI(Tl) Scintillators

An array consisting of two 4”x4”x16” NaI(Tl) scintillators separated by a lead brick wall was used for the measurements. The scintillators were part of two detector systems including enclosures. The cross section from the top is shown in Figure 9.1. The lead wall covered the full height of the scintillators.

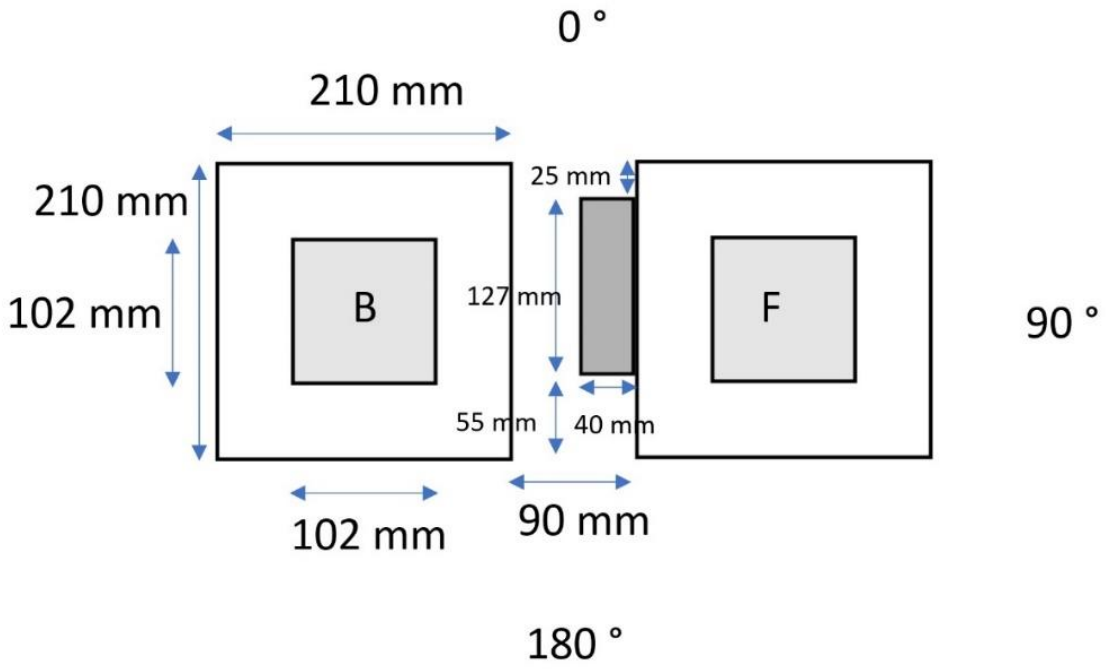

Figure 9.1. Array geometry from above, where F and B indicate the front and back scintillators (grey squares) within their enclosures (larger squares). The darker block in the middle represents the lead brick wall.

Using the dimensions in Figure 9.1, the parameters of the theoretical model are a = 102 mm, b = 102 mm, w= 104 mm and h = 29 mm. A 168 MBq (±10%) Cs-137 source was used for the measurement. The distance from the center of the array to the source was 4.8 m. The gamma spectra were gathered with the detector system’s software. The 662 keV peak areas caused by the Cs-137 source were analyzed with in-house software.

Figure 9.2 presents the angular response of the array compared to the theoretical model. The peak areas were estimated without calculating uncertainties. The measurement live times were several minutes long, and the peak areas where large, with the exception of the measurement of the back detector in the 90 degrees measurement (in this case the peak area estimate was 5300 counts). The statistical uncertainties of the peak areas are thus probably not the main reason for the small deviations from the theoretical model. Errors and uncertainties in the array dimensions, angle and source to array distance probably contribute to the uncertainties and deviations.

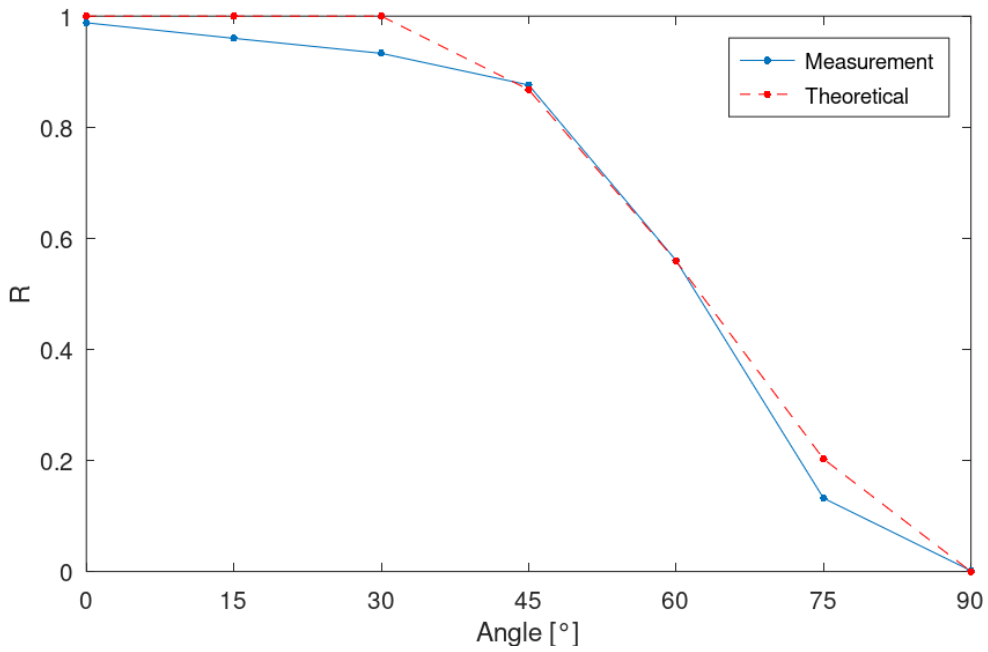

Figure 9.2: Measured and theoretical count rate ratio.

10. Discussion

Source localization is a key performance capability of the relevant authorities in a nuclear accident or nuclear security incident. Several potential technical solutions have been identified (see for examples Guckes et al., 2021; Schrage et al., 2013; Tan et al., 2022), among them being an array of detectors. The simplest array has only two detectors (2x1). It was postulated in the NKS SAMLOC proposal that this structure also potentially provides directional capability. In approaching this problem, three different methodologies were adopted: (1) construction of a simple mathematical geometrical model to estimate the performance capability, (2) verification of the response with Monte Carlo simulations and finally, (3) the performing of experiments using different detector types and sizes.

Two geometrical models were constructed: one for rectangular detectors and one for cylindrical detectors. Then Monte Carlo simulations were performed to compare the response. The results were promising, and the approach appeared valid also for the analysis of real experimental data. These items are considered in the following analyses.

10.1 Geometric Model versus Monte Carlo simulation

The results for Monte Carlo simulations of low-energy photons of Am-241 are almost equal to the predictions of the geometric model (Figure 10.1). The two models represent the same geometric object, a 2x1 CdZnTe array and a Pb shield (see Chapter 5). There is no significant penetration of low-energy photons through the lead shield, even at the edges or corners of the shield. The situation is different for higher energy photons. The data points in Figure 10.2 refer to 661 keV photons of Cs-137. Some of these photons penetrate the front detector and

the Pb shield. To handle this situation, the geometric model, Equation (8), was modified to the form of $R' = R + C$ where the factor C describes the penetration through the shield. In addition, R' was restricted to values between 0 and 1. The modified model gives almost perfect response.

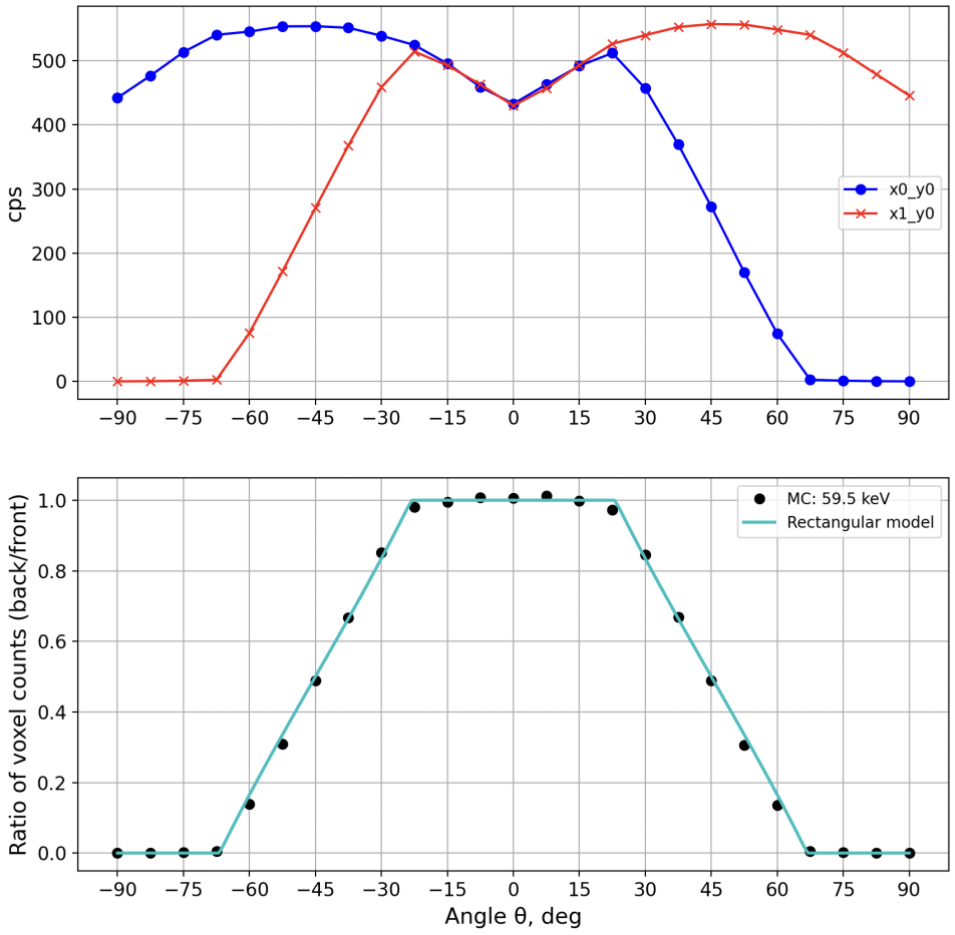

Figure 10.1. Geant4 simulations and the response of the rectangular model in an array consisting of two CdZnTe detectors (see chapter 5). Upper curve: count rate of the detectors labelled as xi_yi. Lower curve: count rate ratio of the detectors considering which one is the front and back detector. Am-241 source with activity of 183 MBq at a distance of 1 m. Model parameters: a = 10 mm, b = 10 mm, w = 10 mm and h = 7.5 mm.

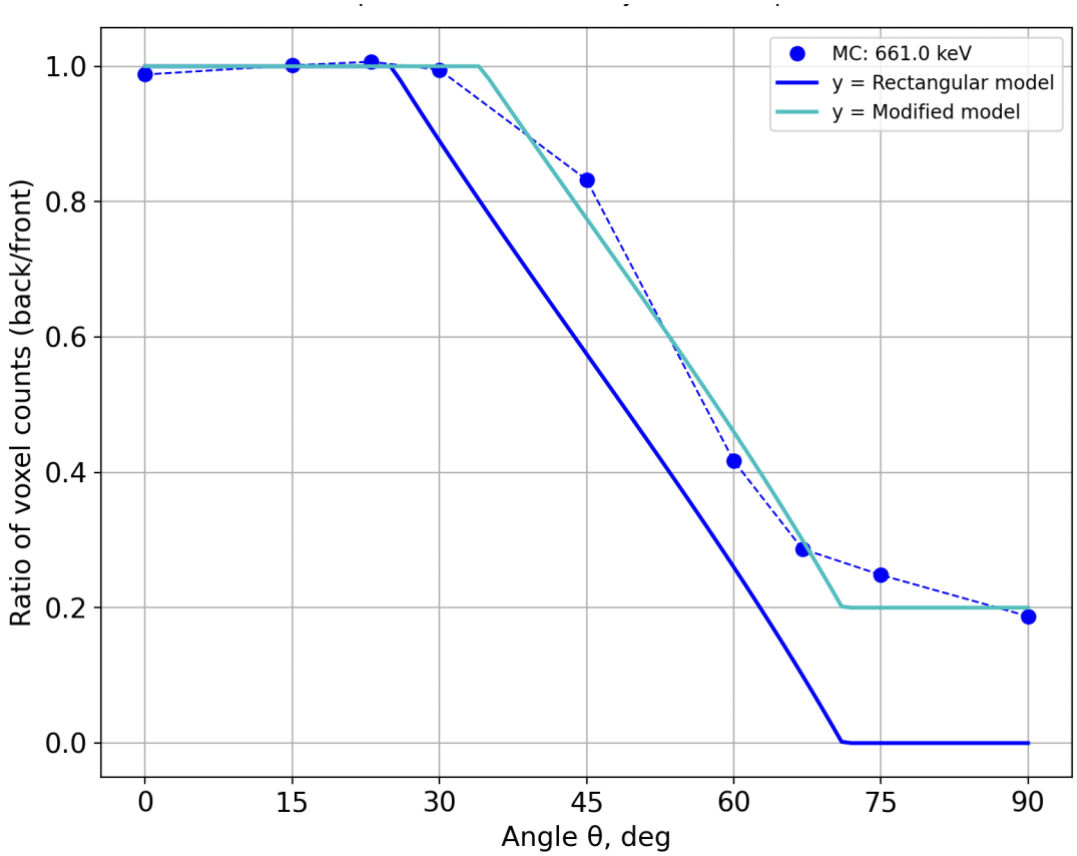

Figure 10.2. Geant4 simulations and the response of the rectangular model for Cs-137 in an array consisting of two CdZnTe detectors (see chapter 5). Model parameters: a = 10 mm, b = 10 mm, w = 10 mm and h = 6 mm. For the modified model, see text (C = 0.2).

10.2 Geometric Model versus experimental results

The 2x1 array has some inherent features which have to be taken into account in the data analysis. The present studies were intended to prove that such an array indeed is useful for source localization. The response was measured as a function of the angle between the source and the array. In principle, the result is a calibration curve in the similar way as is an energy or efficiency calibration of a detector. No inversion was performed, i.e., the data sets were not used for localization of an unknown source. In such an analysis several factors, having an impact on the uncertainty of the source direction, should be considered:

1. Some photons penetrate the shield between the detectors.
2. The front detector may be nearer to the source than the back detector (important at short distances, < 5 m).
3. The source is below or above the vertical surface level of the detectors causing similar exposure component to both detectors.
4. The counting efficiencies of the two detectors are different as a function of angle.
5. The setup is not completely symmetrical (shield installation).
6. Peak area analysis of the acquired data may be difficult, particularly for low statistics.
7. Compton scattering increases the count rate in the region of interest (ROI), and the magnitude of this depends on the environment and source-detector distance.
8. The uncertainty analysis of the ratio of two random variables may be complex because the variables are correlated.

An experimental setup was devised to minimize the impact of the factors listed above. A measurement system with one detector avoids most of the issues. However, then two measurements are required, one with a shield and one without a shield. A heavy lead shield (8 cm) and one large detector (76 mm) eliminates the items detailed in 1, 2, 4 and 5. Items 6 and 7 were handled in peak analysis, acknowledging that the baseline counts are elevated on the left side of the peak. Item 8 was eliminated with very long counting time, providing good statistics. Item 3, the altitude of the array relative to the source is of high importance. If the source is above or below the array, the front windows of both detectors are directly on the source-detector line, thus yielding nuisance primary counts in both detectors. In the measurements, the source and the array were at the same altitude, but this is not necessarily the case in in-field situations. To minimize this phenomenon the entrance of photons through the top and bottom windows should be prevented with additional shielding. Comparing measured data with the cylindrical geometric model shows that in the ideal conditions the model describes reality well (Figure 10.3).

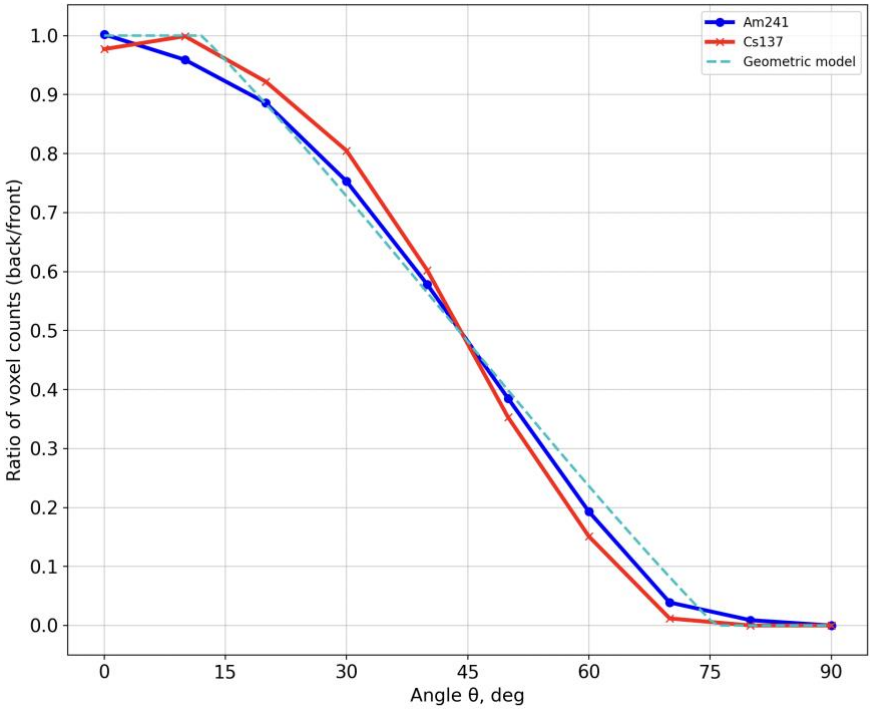

Figure 10.3. Comparison of measurements with the cylindrical model for an array consisting of two cylindrical 3"x3" NaI(Tl) detectors (see chapter 8). Model parameters: r = 38 mm, w = 12 mm and h = 14 mm.

10.3 Data analysis in in-field operations

A straightforward means of analysing unknown field data is to use calibrated count rate ratios for the calculation of the direction of the source relative to the array. First, the measured response data should be smoothed as a function of angle, and then, using interpolation, a look-up table would be calculated for every angle with an accuracy of one degree. The lookup table provides immediately the direction of the source. Additionally, relevant uncertainty analysis routine should be developed noting that the array may have insensitive areas near -90, 0 and 90 degrees. This approach has the advantage that the efficiencies of the two detectors do not have to be equal. In the present study CdZnTe detectors showed some asymmetrical behaviour (see Chapter 5).

If the technical drawings of the detectors are available, then the parameters of the rectangular or the cylindrical model are known, and they can be directly used for the directional calculations. This approach works well for large detectors, dimensions being of the order of 50 mm or more, provided that thick-enough shield is installed between the detectors (4 cm Pb) for high energy photons. The geometric models give best results when the directional insensitive areas are small. This means that the gap between the scintillator surface (or semiconductor surface) and the enclosure of the detector must be small, of the order of a few millimetres.

10.4 Array without any shield between the detectors

All the measurements in the present study were focused on static measurements. These measurements were successful although the gap (w) between the detector and the Pb shield was large (several centimetres). This large gap creates an insensitive range at source directions near angle zero: both detectors record the same count rate for a wide range of angles (± 30 degrees); see Chapters 7 and 9. Modern scintillation detectors can be constructed with a very small gap (a few mm) between the sensitive material and the enclosure of the detector, such as was used in the experiments with 1.5" NaI (Tl) detectors (Chapter 6). Then the insensitive directional area almost disappears.

A 2x1 array without any gap, or a very small gap between the detectors, is well suited for mobile searches with a hand-held instrument. In this mode of operation, the user moves the array direction and keeps an eye on the count ratio between the front and the back detectors. There is no angle calculation; instead, the user tries to find the maximum count ratio. Figure 10.4 shows the response of an idealised bare 2x1 array consisting of two 3" cylindrical NaI detectors touching each other (with no gap between the scintillators). In this case, the maximum count ratio for Cs-137 can achieve a value of 6 or more.

The smaller the energy of the photons, the greater the count ratio observed. In the ideal case of Am-241 this ratio is very large (1000, results not shown). In a real array the detectors are separated by a gap. In principle, this does not reduce the count ratio at the angle of zero degrees (angle α in Figure 2.2). In practise, however, because of difficulties in alignment of the detectors relative to the source, the count ratio may be reduced thus hampering the search effort. Nevertheless, the array is a useful operational tool when connected to a laser pointer or to other support tools to mark the finding.

The gap of zero is an inherent feature of a phoswhich instrument. Then the two detectors are of different materials and therefor their counting sensitivities are not constant. This is not needed in a mobile search operation which is only aimed at finding the direction where the count ratio attains its maximum.

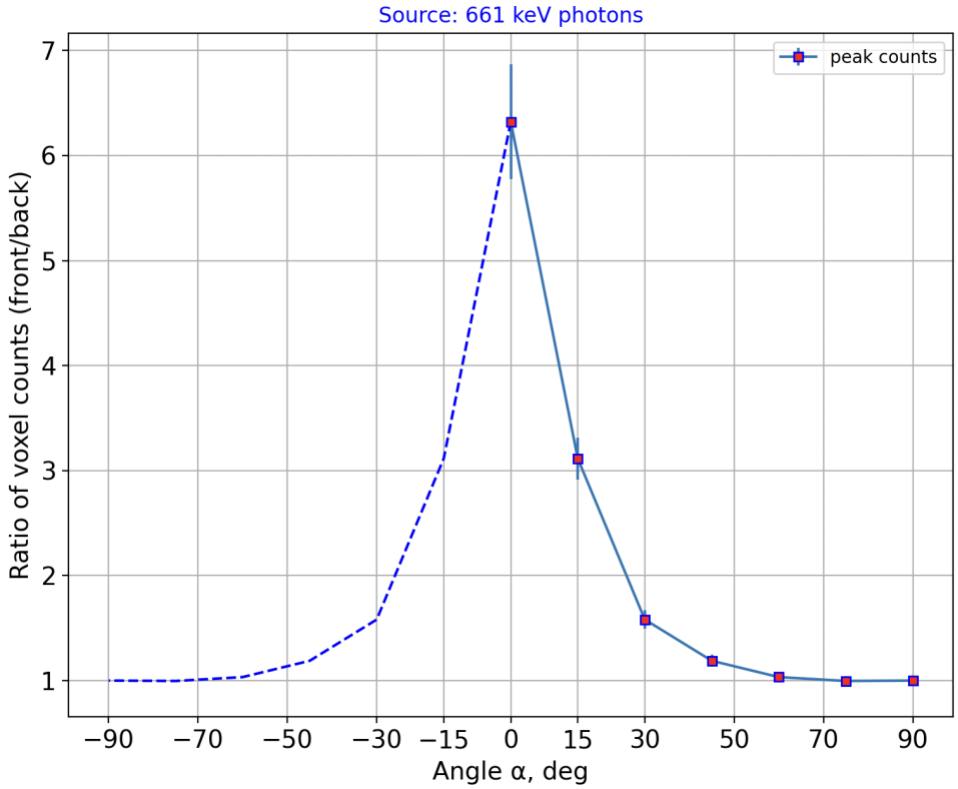

Figure 10.4. Count ratio of two cylindrical 3" NaI detectors touching each other for a simulated 100 MBq Cs-137 source at a distance of 20 m (two-sigma error bars).

11. Conclusions

Simple models, developed for rectangular and cylindrical geometries, explain well the directional data acquired with 2x1 arrays. The models work well for large detectors which provide inherent attenuation of photons in the front detector, preventing them reaching the back detector. A shield of 4 cm Pb between the detectors is enough for a good response (see Chapter 9). Tungsten attenuates photons more efficiently than lead, and is therefore an ideal material for the shield, but it is more expensive limiting its usage to small arrays.

A 2x1 array has a field of view of 180 degrees. A serious mistake may take place in the field missions, unless this issues is properly treated. A solution is an additional shield on the back side of the array, or the problem is solved operationally utilizing local information on the possible locations of the unknown source.

Comparison measurements were performed between 2x1 and 2x2 arrays (Chapter 6). The latter is technically superior having 360 degrees field of view, and there is no need to perform any modelling of the array; the acquired data as such are enough for reliable source localization with an accuracy better than 10 degrees for all directions (Toivonen et al., 2024). However, a 2x1 array is technically much simpler and cheaper, albeit with lower directional accuracy. The array suits well for surveillance of an area of interest. Such situations are relevant in nuclear security, for example in border control, sports events, and high-level political summits.

12. References

Agostinelli, S., Allison, J., Amako, K.A., Apostolakis, J., Araujo, H., Arce, P., Asai, M., Axen, D., Banerjee, S., Barrand, G.J.N.I. and Behner, F., 2003. GEANT4—a simulation toolkit. Nuclear instruments and methods in physics research section A: Accelerators, Spectrometers, Detectors and Associated Equipment, 506(3), pp.250-303. https://doi.org/10.1016/S0168-9002(03)01368-8

Guckes, A., Barzilov, A., Guss, P., 2021. Experimental study of directional detection of neutrons and gamma rays using an elpasolite scintillator array. Nucl. Instrum. Methods Phys. Res., Sect. A 992. https://doi.org/10.1016/j.nima.2021.165028.

Schrage, C., Schemm, N., Balkir, S., Hoffman, M.W., Bauer, M., 2013. A low-power directional gamma-ray sensor system for long-term radiation monitoring. IEEE Sensor. J. 13, 2610–2618. https://doi.org/10.1109/JSEN.2013.2258009

Shirakawa, Y., Yamano, T., Kobayashi, Y., 2009. Remote sensing of nuclear accidents using a directionfinding detector, 2009. In: IECON Proceedings (Industrial Electronics Conference), pp. 1917–1922. https://doi.org/10.1109/ IECON.2009.5414850

Tan, W., Zhou, J., Fang, F., Li, X., Hong, X., 2022. A fast gamma-ray source localization method for mobile robots. Appl. Radiat. Isot. 188, 110377 https://doi.org/10.1016/ j.apradiso.2022.110377

Toivonen, H., Dowdall, M., Ihantola, S. Novel In-field Technologies for Source Localization. NKS workshop, Helsinki, September, 2023. Available at: https://docs.google.com/presentation/d/1p9VsJmlcpTcZaU2qQDrBphuSSh_QfvIZ/edit?usp=sharing&ouid=101337960941938456970&rtpof=true&sd=true

Toivonen, H., Dowdall, M., Ihantola, S. 2024. On the symmetry of photon detection arrays: A directionally sensitive 3D model, Applied Radiation and Isotopes, 206,111219, https://doi.org/10.1016/j.apradiso.2024.111219

Bibliographic Data Sheet **NKS-505**

Title	Symmetrical Array Methodology for Gamma Source Localization: Technology Transfer Workshop and Field Event (SAMLOC)
Author(s)	Harri Toivonen[1] Mark Dowdall[2] Sakari Ihantola[3] Gísli Jónsson[4], Pernille Ahlmann Jensen[4] Jussi Huikari[5], Kari Peräjärvi[5], Philip Holm[5] Aliaksandr Dvornik[6], Maria Karampiperi[6], Christopher Rääf[6], Viktor Lehmann[6], Robert Finck[6], Christian Bernhardsson[6]
Affiliation(s)	[1]HT Nuclear Oy, 05880 Hyvinkää, Finland, [2]Norwegian Radiation and Nuclear Safety Authority, 1361, Østerås, Norway, [3]Radis Technologies Oy, Finland, [4]Icelandic Radiation safety Authority, 105 Reykjavík, Iceland, [5]Radiation and Nuclear Safety Authority, 01370 Vantaa, Finland,[6]Lund University, Malmö, Sweden
ISBN	978-87-7893-603-5
Date	October 2025
Project	NKS-B / SAMLOC - AFT/B(24)4
No. of pages	37
No. of tables	2
No. of illustrations	41
No. of references	7

Abstract
max. 2000 characters

Effective response to incidents involving searches for nuclear or other radioactive materials out of regulatory control (MORC) is dependent on rapid localization of the source, which is often hindered due to a general lack of available, efficient, robust directionally sensitive detector systems designed for field and security applications. The SAMLOC project assembled Nordic expertise in this area to test new developments, exchange technologies and experience and enhance Nordic capacities in this field. The primary objective of SAMLOC was is to investigate the application of the symmetrical array method to detector types employed in the Nordic region and to test this and conventional methods in tests of directional estimation. The project demonstrated that simple models, developed for rectangular and cylindrical detector geometries, explain well the directional data acquired with 2x1 arrays of detectors. The models function well for large detectors which provide inherent attenuation of photons in the front detector, preventing them reaching the back detector. A shield of 4 cm Pb between detectors was sufficient for a good directional response. Comparison measurements were performed between 2x1 and 2x2 arrays. The latter was technically superior having 360 degrees field of view, and there was no need to perform any modelling of the array. However, a 2x1 array is technically much simpler and cheaper, albeit with lower directional accuracy. The array is well suited for

static surveillance of an area of interest and is of relevance in nuclear security applications.

Key words: Gamma spectrometry, detector arrays, source locations, directionality